

1 **Bacterial defences interact synergistically by disrupting phage cooperation**

2

3 Alice Maestri<sup>1</sup>, Elizabeth Pursey<sup>1#</sup>, Charlotte Chong<sup>2#</sup>, Benoit J. Pons<sup>1</sup>, Sylvain Gandon<sup>3</sup>, Rafael  
4 Custodio<sup>1</sup>, Matthew Chisnall<sup>1</sup>, Anita Grasso<sup>1,4</sup>, Steve Paterson<sup>2</sup>, Kate Baker<sup>2</sup>, Stineke van Houte<sup>1</sup>, Anne  
5 Chevallereau<sup>5\*</sup>, Edze R. Westra<sup>1\*</sup>

6

7 <sup>1</sup> Environment and Sustainability Institute, Biosciences, University of Exeter, Penryn TR10 9FE, UK

8 <sup>2</sup> Institute of Infection, Veterinary and Ecological Sciences, University of Liverpool, Liverpool L69  
9 3BX, UK

10 <sup>3</sup> CEFÉ, CNRS, Université de Montpellier, EPHE, IRD, Montpellier 34293, France

11 <sup>4</sup> Department of Comparative Biomedicine and Food Science, Università degli Studi di Padova, Padova  
12 35020, Italy (current affiliation)

13 <sup>5</sup> Université Paris Cité, CNRS, INSERM, Institut Cochin, Paris F-75014, France

14

15 <sup>#</sup>\*These authors contributed equally

16 Correspondence to: anne.chevallereau@inserm.fr; E.R.Westra@exeter.ac.uk

17

18 **Summary**

19 The constant arms race between bacteria and their phages has resulted in a large diversity of bacterial  
20 defence systems<sup>1,2</sup>, with many bacteria carrying several systems<sup>3,4</sup>. In response, phages often carry  
21 counter-defence genes<sup>5–9</sup>. If and how bacterial defence mechanisms interact to protect against phages  
22 with counter-defence genes remains unclear. Here, we report the existence of a novel defence system,  
23 coined MADS (Methylation Associated Defence System), which is located in a strongly conserved  
24 genomic defence hotspot in *Pseudomonas aeruginosa* and distributed across Gram-positive and Gram-  
25 negative bacteria. We find that the natural co-existence of MADS and a Type IE CRISPR-Cas adaptive  
26 immune system in the genome of *P. aeruginosa* SMC4386 provides synergistic levels of protection  
27 against phage DMS3, which carries an anti-CRISPR (*acr*) gene. Previous work has demonstrated that  
28 Acr-phages need to cooperate to overcome CRISPR immunity, with a first sacrificial phage causing host  
29 immunosuppression to enable successful secondary phage infections<sup>10,11</sup>. Modelling and experiments  
30 show that the co-existence of MADS and CRISPR-Cas provides strong and durable protection against  
31 Acr-phages by disrupting their cooperation and limiting the spread of mutants that overcome MADS.  
32 These data reveal that combining bacterial defences can robustly neutralise phage with counter-defence  
33 genes, even if each defence on its own can be readily by-passed, which is key to understanding how  
34 selection acts on defence combinations and their coevolutionary consequences.

35

## 1 **Introduction**

2 Phage are important drivers of the ecology and evolution of their bacterial hosts<sup>12</sup>. In response to phage  
3 predation, bacteria have evolved many different defence systems, such as Restriction-Modification  
4 (RM) and CRISPR-Cas<sup>13</sup>. Crucially, literally dozens of previously unknown defences were discovered  
5 in recent years<sup>2,14-19</sup>, often aided by their clustering in defence islands<sup>20,21</sup>. These defence systems  
6 frequently coexist in the same genome<sup>20-23</sup>, which can prevent the emergence of spontaneous phage  
7 mutants that overcome host resistance. For example, the co-occurrence of a Type I BREX and Type IV  
8 RM systems prevents the emergence of epigenetic mutants that overcome BREX, since these are cleaved  
9 by the Type IV RM system<sup>24</sup>, and the co-existence of RM and CRISPR-Cas leads to a reduction in the  
10 frequency of spontaneous phage mutants that escape both defences as well as a higher rate of CRISPR  
11 immunity acquisition<sup>25,26,27</sup>. However, many phage can employ more sophisticated counter-defence  
12 mechanisms, such as anti-RM<sup>5</sup>, anti-CRISPR (Acr)<sup>6</sup> and the more recently identified anti-CBASS<sup>7,8</sup>,  
13 anti-Pycsar<sup>8</sup> and anti-TIR-STING<sup>9</sup> proteins. We currently lack an understanding of how multi-layered  
14 bacterial defences impact the efficacy and deployment of these sophisticated phage counter-defence  
15 systems, and how this influences bacteria-phage coevolution. Previous work on the epidemiological and  
16 co-evolutionary consequences of Acr-phage infections has demonstrated that Acr are imperfect,  
17 resulting in a high proportion of failed infections of CRISPR-immune bacteria<sup>6</sup>. This imperfection is at  
18 least in part due to Acr production taking place after infection (i.e., Acr are not packaged into the phage  
19 capsid)<sup>6,28</sup>, whereas CRISPR immune complexes are already present in the cell upon infection. Because  
20 of this, Acr-phages must cooperate to overcome CRISPR immunity: the production of Acr proteins by  
21 a first sacrificial phage into a CRISPR immune host cell is necessary to enable a second Acr-phage to  
22 successfully infect the same host<sup>10,11</sup>. As a consequence, Acr-phages can amplify only if their density  
23 exceeds a critical threshold that supports the required frequency of secondary infections. However, our  
24 understanding of these dynamics is currently limited to the simple scenario where CRISPR-Cas immune  
25 systems are the sole resistance determinants, and it is unclear if and how this may be impacted by the  
26 presence of other defence genes in the bacterial genome.

27

## 28 **Results**

### 29 **Bacteria drive Acr-phages extinct**

30 We aimed to study how the Type IE CRISPR-Cas immune system of *P. aeruginosa* SMC4386 shapes  
31 the coevolutionary interactions with its phage DMS3. The CRISPR-Cas immune system of this bacterial  
32 strain carries a spacer that perfectly matches the genome of DMS3, whereas the phage carries an anti-  
33 CRISPR gene (*acrIE3*) that blocks the Type IE CRISPR-Cas system<sup>29</sup>. However, infection experiments  
34 of *P. aeruginosa* SMC4386 with phage DMS3<sup>vir</sup>, a c-repressor mutant locked in the lytic cycle, revealed  
35 that, although phages successfully adsorbed to the bacteria (Extended Data Fig. 1a), they were unable to

1 amplify and instead rapidly went extinct, even at high initial multiplicity of infection (MOI) (Extended  
2 Data Fig. 1b). Moreover, infection experiments with the temperate phage DMS3-Gm, a mutant of phage  
3 DMS3 that carries a gentamycin resistance gene<sup>11</sup> which allows the selection for lysogens, revealed that  
4 no lysogens were formed in the SMC4386 strain, while lysogens could be observed for the reference  
5 PA14 strain (Extended Data Fig. 1c). The absence of lysogen formation in SMC4386 contrasts with  
6 previous work showing efficient lysogenization on bacteria with CRISPR-Cas immunity when phages  
7 carry *acr* genes<sup>6,11,30</sup>.

8 Previous studies have shown that Acr proteins are imperfect and vary in their strength, ranging  
9 from highly effective to weak inhibitors of CRISPR-Cas<sup>10,11</sup>. If AcrIE3 was a weak inhibitor of CRISPR-  
10 Cas, it would explain the lack of phage amplification or lysogen formation on CRISPR immune bacteria.  
11 To test this hypothesis, we compared the efficiency of plating (EOP) of phage DMS3vir and a phage  
12 mutant lacking the *acrIE3* gene (referred to as DMS3virΔ*acr*). While DMS3vir could form plaques on  
13 SMC4386, DMS3virΔ*acr* could not, supporting the hypothesis that AcrIE3 efficiently blocks the Type  
14 IE CRISPR-Cas immune system of SMC4386 (Extended Data Fig. 1d). Consistent with this observation,  
15 phage DMS3virΔ*acr* was able to form plaques on a CRISPR-Cas deletion mutant (SMC4386ΔCRISPR,  
16 referred to as ΔCRISPR) (Extended Data Fig. 1d). Moreover, unlike DMS3virΔ*acr*, we did not detect  
17 an increase in DMS3vir EOP on the ΔCRISPR strain compared to the wildtype SMC4386 (SMC4386-  
18 WT) (Fig. 1a, compare yellow and black bars). Collectively, these data suggest that AcrIE3 is an  
19 effective inhibitor of the Type IE CRISPR-Cas system of *P. aeruginosa* SMC4386.

## 20 A novel defence system coined MADS

21 Based on these observations, we hypothesised that *P. aeruginosa* SMC4386 may carry additional  
22 defence systems that limit DMS3 infectivity. To test this prediction, we generated a transposon (Tn)  
23 mutant library of SMC4386-WT, which we then infected with DMS3-Gm. Interestingly, lysogen  
24 formation was observed in the SMC4386-Tn mutant library (Extended Data Fig. 2c, yellow line), but  
25 not in the SMC4386-WT strain (Extended Data Fig. 1c). PCR analysis of the DMS3 c-repressor gene  
26 confirmed that 83.6% of the Gm-resistant clones within the SMC4386-Tn mutant population were  
27 lysogens, and not spontaneous Gm-resistant mutants. Sanger sequencing of these lysogens revealed that  
28 most of the Tn insertions were located in *cas* genes (Extended Data Fig. 2b), supporting the idea that  
29 Acr proteins are imperfect and that CRISPR-Cas plays a role in blocking DMS3 lysogen formation,  
30 despite the phage carrying an *acrIE3* gene. To test the hypothesis that additional genes, beyond CRISPR-  
31 Cas, are involved in defence against phage DMS3, we next generated a transposon mutant library of the  
32 ΔCRISPR strain. Using the same method, we identified multiple Tn insertions in a restricted genomic  
33 region containing a predicted operon of 8 genes<sup>31,32</sup> (Extended Data Fig. 2c). This putative operon did  
34 not contain a known defence system based on PADLOC and DefenseFinder analyses<sup>3,33</sup> (Supplementary  
35 Table 1). However, PADLOC identified 3 genes in this operon as putative components of DNA-

1 modification systems: a kinase, a specificity subunit and a methylase (Supplementary Table 1).  
2 Therefore, we hypothesised that this operon might encode a defence system that has not been previously  
3 described, which we coined MADS (Methylation Associated Defence System) (Fig. 1b). Interestingly,  
4 this putative new 8-gene system contains predicted domains that are also found in other bacterial defence  
5 systems (see Supplementary Notes), supporting a role in defence against mobile genetic elements (MGE)  
6 (Fig. 1b). To experimentally test this hypothesis, we knocked out ~22kb of the genome encompassing  
7 this operon (referred to as  $\Delta$ MADS). Plaque assays with phage DMS3vir showed a 100-fold increase in  
8 the EOP on  $\Delta$ MADS compared to the WT strain (Fig. 1a, orange bar). Likewise, the EOP of  
9 DMS3vir $\Delta$ acr increases by approximately 100-fold on a double mutant  $\Delta$ MADS $\Delta$ CRISPR compared to  
10  $\Delta$ CRISPR (Fig. 1a, compare yellow and green bars). The observed differences in phage infectivity were  
11 reflected in the suppression of bacterial growth in the presence of phages. When MADS is not present  
12 ( $\Delta$ CRISPR $\Delta$ MADS and  $\Delta$ MADS strains), bacteria displayed normal growth in the absence of phage  
13 DMS3vir but reduced growth in its presence (Fig. 1c, orange and green curves), whereas in the presence  
14 of MADS (WT and  $\Delta$ CRISPR strains) bacteria grew equally well in the presence and absence of phage  
15 at a MOI of 10 (Fig. 1c, black and yellow curves).

16 Having established that this operon encodes a novel defence system, we next wanted to test the  
17 implication of each gene in this phenotype (*mad1-8*, Fig. 1b). We therefore generated knock-out mutants  
18 of each individual gene and measured how this impacted the phage resistance. Interestingly, despite  
19 repeated attempts, we were unable to delete *mad5*, unless also *mad2* or *mad3* were deleted, suggesting  
20 that deletion of *mad5* alone is lethal. Infection experiments showed that individual gene deletions of  
21 *mad2-4* and *mad6-8* all resulted in reduced bacterial growth in the presence of phage DMS3vir, whereas  
22 deletion of *mad1* had limited effect (Fig. 1d). Moreover, deletion of either the full system or each of the  
23 individual *mad* genes resulted in a 30- to 400-fold increase in phage DMS3 lysogen formation in mutant  
24 backgrounds relative to the  $\Delta$ CRISPR strain, except for *mad1* (Fig. 1e). To understand the range of  
25 protection offered by MADS, we carried out infection assays with diverse phages, including temperate  
26 phage LPB1(*Casadabanvirus*) and lytic phages LMA2 (*Pbunavirus*) and LUZ24 (*Bruynoghevirus*). We  
27 observed a similar increase (>10-fold) in the EOP of all phages in  $\Delta$ MADS strain relative to the  
28 SMC4386-WT (Fig. 1f). Based on these data, we conclude that the MADS system encodes a novel  
29 defence system that is active against at least 4 different phages, with genes *mad2-4* and *mad6-8* being  
30 essential for phage resistance.

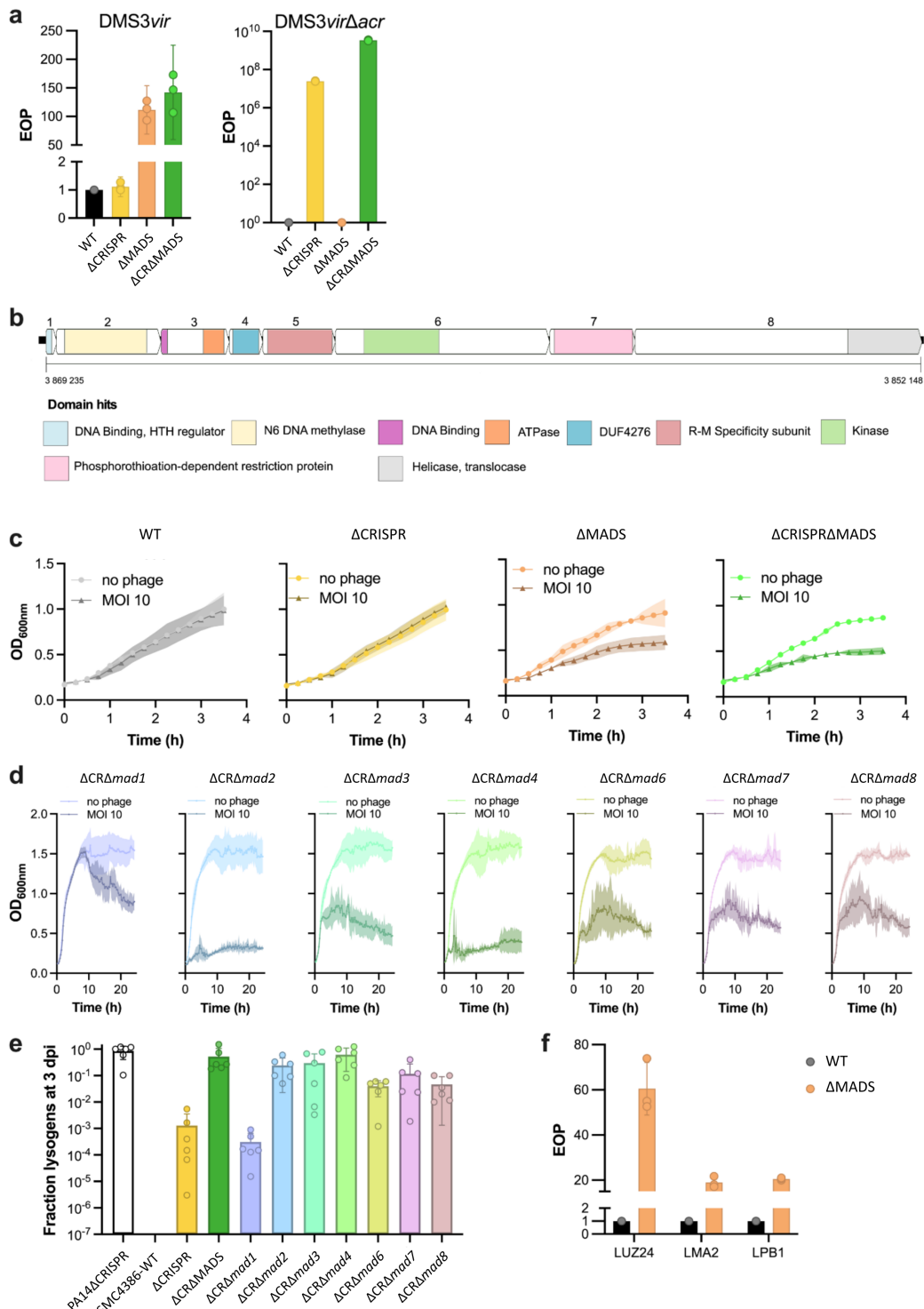


**Fig. 1 | MADS protects bacteria against phages.** **a**, Efficiency of plating (EOP) of phage DMS3vir or DMS3virΔacr on strains SMC4386-WT, ΔCRISPR, ΔMADS and ΔCRISPRΔMADS. **b**, MADS is an 8-gene operon. Numbers in the top arrows correspond to gene numbering (*mad1-mad8*). Colours in bottom arrows indicate domain hits predicted with HHpred analyses and the scale indicates the position of the *mad* operon on the SMC4386 genome assembled as single chromosome (in bp). **c, d**, Bacterial growth curves of WT and mutant strains in absence or presence of phage DMS3vir (with multiplicity of infection, MOI, of 10). Single *mad* gene deletions are all in a ΔCRISPR background (indicated as ΔCRΔmad $X$ , with  $X$  the gene number). **e**, Fraction of the bacterial population carrying the DMS3 prophage (lysogens) in WT and mutant SMC4386 backgrounds, as indicated. ΔCR is an abbreviation for ΔCRISPR. **f**, EOP of phages LUZ24, LMA2 and LPB1 on SMC4386-WT and the isogenic ΔMADS strain. For each panel, values for individual replicates are shown (3 replicates in panels a and f, 4 replicates in c and d and 6 replicates in panel e) as well as mean values. Errors bars (panels a, e, f) and shaded areas (panels c, d) show 95% confidence intervals (c.i.).

1 **Distant bacterial classes carry MADS**

2 To determine how widespread and conserved MADS is, we built a MacSyFinder model<sup>34</sup> and searched  
3 through all bacterial and archaeal genomes in the RefSeq database. We identified 422 MADS in 100  
4 different species belonging to *Alpha*, *Beta*, *Gamma* and *Deltaproteobacteria*, *Actinobacteria* and  
5 *Nostocales* (Extended Data Fig. 3a). The *madI-8* operon was most commonly found in the genera  
6 *Escherichia* (n=113, 27% of systems detected), *Pseudomonas* (n=71, 17%), *Ralstonia* (n=51, 12%),  
7 *Streptomyces* (n=33, 8%), *Klebsiella* (n=31, 7%) and *Vibrio* (n=15, 4%) (Extended Data Fig. 3b). This  
8 analysis also revealed varying levels of completeness of MADS operon, with some genes missing or  
9 being detected less frequently in some bacterial genera, suggesting the existence of multiple subtypes of  
10 MADS (Extended Data Fig. 3c,d). The majority of operons identified in the search contained 8 or more  
11 genes, including multiple hits to the same gene type, possibly reflecting gene duplication events  
12 (Extended Data Fig. 3e).

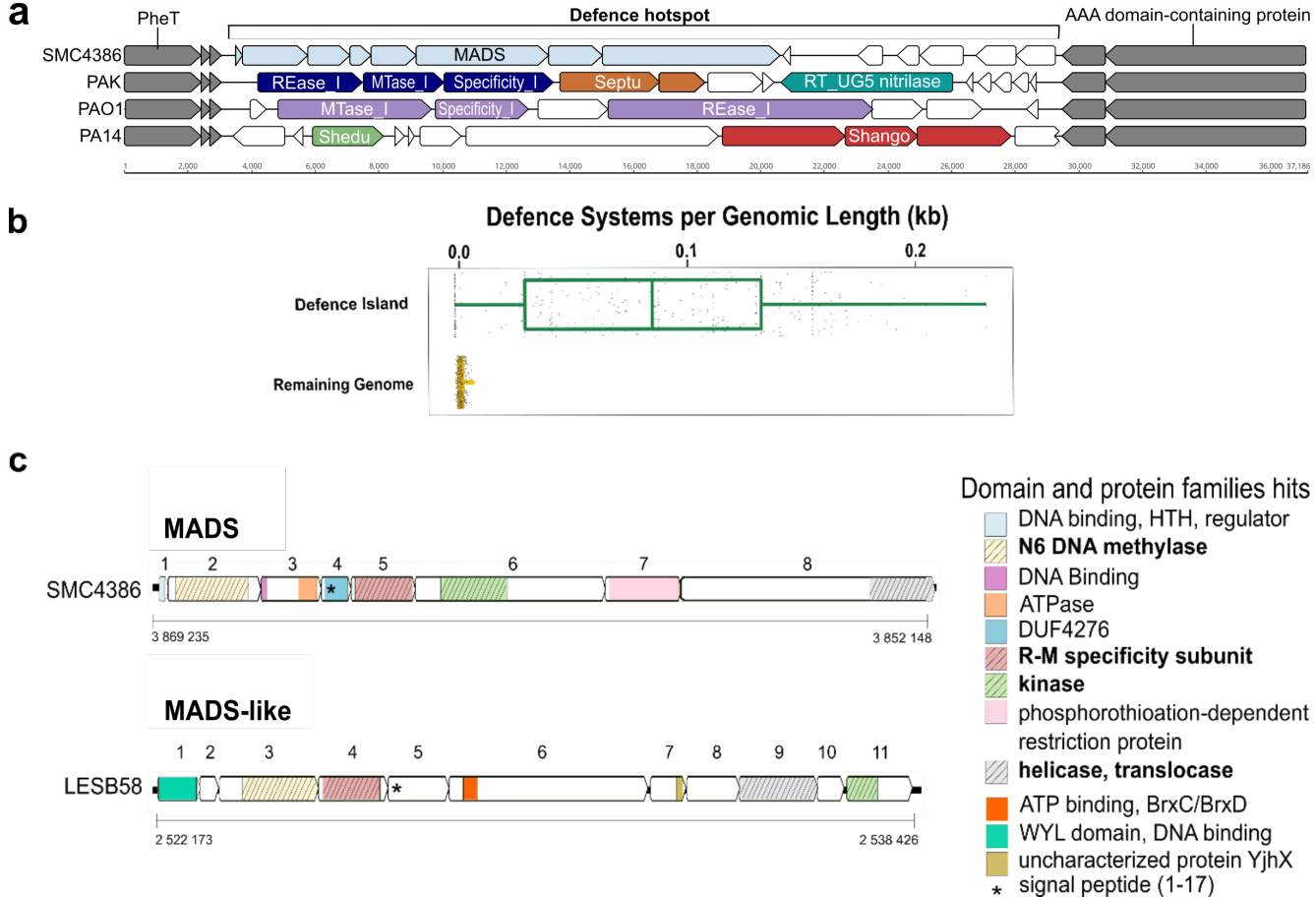
13

14 **MADS is located in a defence hotspot**

15 A deeper examination of the *P. aeruginosa* genomes containing MADS revealed that the complete  
16 operon was detected in approximately 1% (66/6103) of the genomes analysed. Interestingly, manual  
17 inspection of these 66 genomes led to the observation that in at least 51/66 (77%), the MADS operon  
18 was located within a genomic region with conserved gene boundaries: *pheT*, a phenylalanine tRNA  
19 ligase subunit beta (MPAO1\_RS11510) and a histidine kinase (MPAO1\_RS11445). An extended search  
20 encompassing all the currently available complete *P. aeruginosa* genomes (n= 454) revealed a highly  
21 conserved hotspot for *P. aeruginosa* defence systems at this location in the genome (Fig. 2a). The gene  
22 boundaries were found in 97% (444/454) of the genomes analysed (Supplementary Table 2), delimiting  
23 genomic islands with sizes ranging from 9.5 kb to 2402.9 kb, with an average length of 64.3 kb. For the  
24 444 genomes containing the island, PADLOC<sup>33</sup> was used to annotate defence systems both on the  
25 extracted islands (Supplementary Table 3) and on the remainder of the genome (Supplementary Table  
26 3). Analysing the number of defence systems detected by PADLOC per unit of genomic length (in kb)  
27 confirmed a statistically significant enrichment for defence systems on this island, with a median of 0.1  
28 systems/kb in the defence island and 0.003 systems/kb in the remainder of the genome (Fig. 2b,  
29 Wilcoxon's signed rank test, p<0.05). Further analysis revealed that this island contains at least one  
30 defence system in 81% (358/444) and two or more defence systems in 78% (346/444) of all genomes  
31 analysed, with a total of 46 different known defence systems, as well as potential novel or incomplete  
32 defence systems (Extended Data Fig.4a and Supplementary Notes). Manual inspection of such systems  
33 revealed a putative novel defence system related to the MADS system that we coined 'MADS-like': this  
34 is a 11-gene system (numbered *madI1* to *madI11*), which was found in 10/444 islands (Fig. 2c, Extended  
35 Data Fig.4b and Supplementary Notes). Interestingly, both MADS and the MADS-like are predicted to  
36 encode a N6-Methyltransferase (Fig. 2c and Supplementary Notes), which suggests that self/non-self

1 discrimination relies on a methylation-based mechanism, a common strategy employed by many  
2 bacterial innate immune systems, such as Restriction-Modification, BREX and DISARM<sup>35</sup>.

3



4

5 **Fig. 2 | MADS is located in an integration hotspot for bacterial defence systems.** **a**, Composition of the  
6 genomic island in strains SMC4386, PAK, PAO1 and PA14. Conserved genes forming the boundaries of the  
7 island are indicated in grey. Coloured arrows indicate genes forming indicated defence systems. **b**, Number of  
8 defence systems per genomic length (kb) in the defence island compared to the remaining genome. Boxplots  
9 display the interquartile range, median and maximum defence systems per genomic length (kb) in the defence  
10 island and the remaining genome. Each grey dot represents density values for each isolate. **c**, Comparison of the  
11 MADS and MADS-like putative defence systems. Predicted protein domains (HHpred) are indicated with  
12 coloured boxes. Protein domains that are common between MADS and MADS-like are indicated in bold  
13 characters.

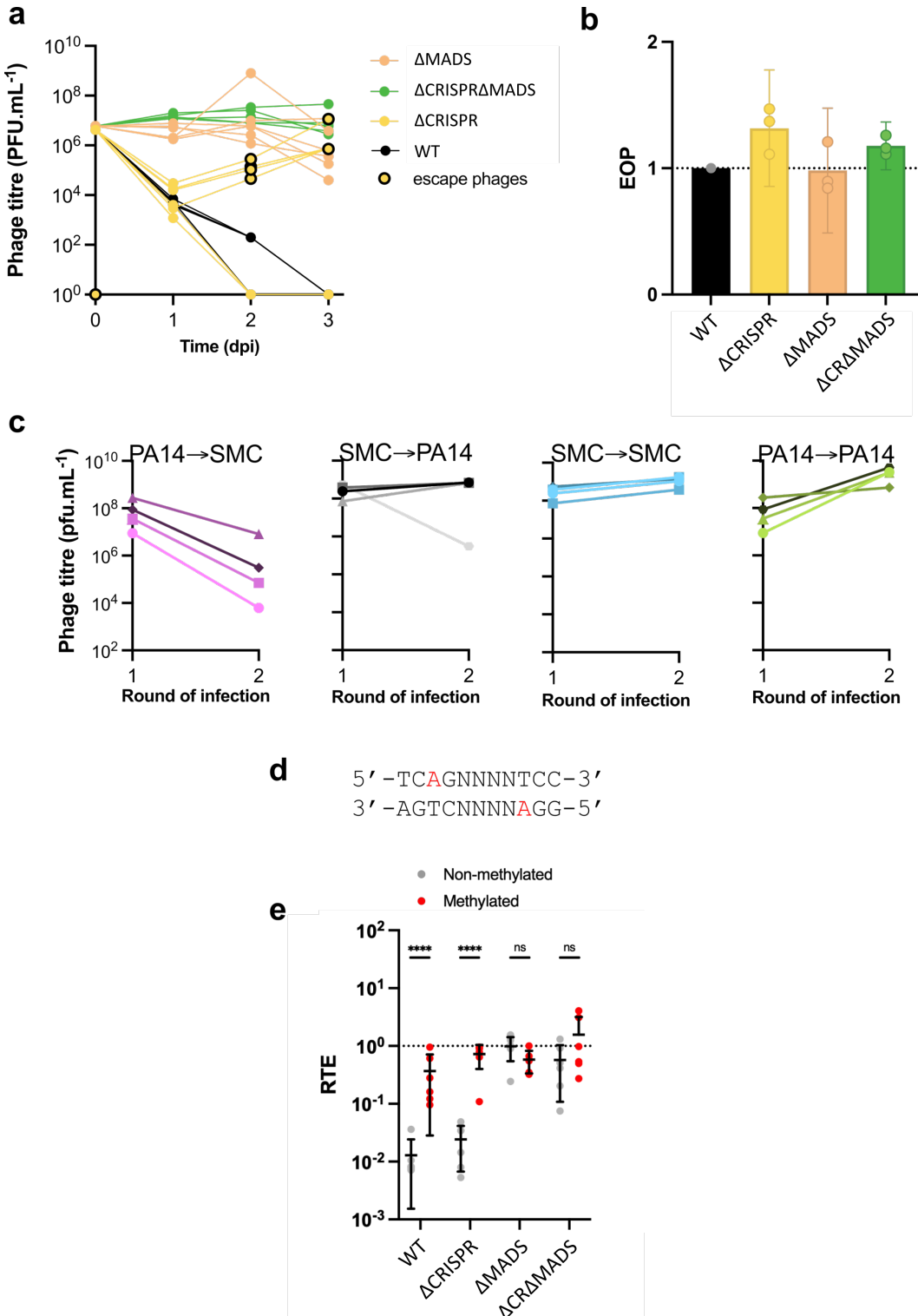
14

## 15 Epigenetic phage mutants escape MADS

16 To test whether MADS uses epigenetic modification for self/non-self discrimination, we co-cultured  
17 phage DMS3vir and SMC4386ΔCRISPR, and monitored whether phages could evolve to overcome  
18 MADS. When the ΔCRISPR strain was infected with phage DMS3vir, we noticed that in some of the  
19 replicates, the phage population amplified after 2 days of infection (Fig. 3a, yellow circles with black  
20 outline). This indicates that in the absence of CRISPR-Cas, some phages evolved to overcome MADS.  
21 Interestingly, such ‘escape’ phages did not emerge during infection of the WT strain, suggesting a  
22 synergistic effect of CRISPR-Cas and MADS that prevents the evolutionary emergence of phage escape  
23 variants (Fig. 3a, black lines). The phages that evolved to overcome MADS were isolated and their

1 infectivity was measured on different SMC4386 mutant backgrounds. This test revealed that they formed  
2 plaques with equal efficiency on all genomic backgrounds (WT,  $\Delta$ CRISPR,  $\Delta$ MADS and  
3  $\Delta$ CRISPR $\Delta$ MADS strains, Fig 3b). To test whether the modification which allowed these escape phages  
4 to overcome MADS was epigenetic, we next amplified these phages successively on PA14 $\Delta$ CRISPR  
5 (which lacks MADS) and on SMC8346-WT strains. We predicted that during amplification in the PA14  
6 background, escape phages would lose the epigenetic modification that underpins their ability to bypass  
7 MADS, and hence lose their ability to infect SMC4386-WT in a successive passage. Consistent with  
8 this hypothesis, phages that replicated on PA14 $\Delta$ CRISPR had a decreased infectivity when they were  
9 next passaged on the SMC4386-WT strain (Fig. 3c, PA14 $\rightarrow$ SMC), whereas this was not the case if they  
10 replicated on the SMC4386-WT strain in the previous round of infection (Fig 3c, SMC $\rightarrow$ PA14) or if  
11 they replicated on the same strain in the previous round of infection (Fig. 3c, SMC $\rightarrow$ SMC,  
12 PA14 $\rightarrow$ PA14).

13 To corroborate these phenotypic analyses and to identify the epigenetic modification site, we  
14 carried out PacBio sequencing of the escape phages and the ancestral DMS3 $vir$  phage. Sequencing  
15 results revealed that the motif 5'-TCAGNNNNNTCC-3' has m6A modifications at positions 3 and 9 on  
16 the positive and negative strands, respectively, in the escape phage, but not in the ancestral phage  
17 genome (Fig. 3d). The phage has 7 such motifs, all of which were methylated in the escape phages.  
18 Moreover, PacBio sequencing of the bacterial DNA revealed that the same motifs were methylated on  
19 the bacterial chromosome in the SMC4386-WT and  $\Delta$ CRISPR strains, whereas these sites were not  
20 methylated in the  $\Delta$ CRISPR $\Delta$ MADS, nor in the  $\Delta$ CRISPR $\Delta$ mad2 strain, which encodes the predicted  
21 methyltransferase. The combination of phenotypic and sequencing data therefore supports the  
22 hypothesis that MADS uses a methylation-based self/non-self discrimination mechanism. To further  
23 corroborate the hypothesis that MADS provides resistance against MGE with unmethylated 5'-  
24 TCAGNNNNNTCC-3' sequence, but not against MGE with a methylated sequence, we measured the  
25 transformation efficiency of methylated and unmethylated plasmids with the target sequence relative to  
26 a plasmid without this sequence. Consistent with our hypothesis, a methylated plasmid carrying a 5'-  
27 TCAGCGCGTCC -3' sequence had a 100-fold increased relative transformation efficiency (RTE)  
28 compared to the non-methylated plasmid when recipient cells carried MADS (SMC4386-WT or  
29 SMC4386 $\Delta$ CRISPR, Fig. 3e), while no differences could be observed when strains lacked MADS  
30 ( $\Delta$ MADS or  $\Delta$ CRISPR $\Delta$ MADS). Overall, our data show that recognition of the unmethylated 5'-  
31 TCAGCGCGTCC -3' sequence by MADS is required for mediating resistance against infections by  
32 MGE.



1

2 **Fig. 3 | Phages escape MADS through epigenetic modification.** **a**, Titre of phage DMS3vir over 3 days post  
3 infection (MOI 0,1) of strains SMC8386-WT, ΔCRISPR, ΔMADS or ΔCRISPRΔMADS. Yellow circles with  
4 black outline indicate replicates from which DMS3vir escape phage mutants were isolated. Data are shown for 6  
5 individual replicates. **b**, EOP of DMS3vir escape mutants (isolated in the experiment shown in panel a) measured  
6 on indicated strains. Individual and mean data are shown for 3 individual replicates. Error bars show 95%  
7 confidence intervals (c.i.). **c**, Amplification patterns of DMS3vir escape mutants when successively passaged on  
8 PA14ΔCRISPR and SMC4386-WT, with the order of passaging indicated on top of the graphs. Phage titre was  
9 assessed after each round of amplification using spot assay on PA14ΔCRISPR. Each panel shows data obtained  
10 with four independent escape phages (isolated in the experiment shown in panel a). **d**, Sequence of the genomic  
11 site that is modified by the MADS system. Adenosines that are methylated at positions 3 and 9 on the positive  
12 and negative strands (respectively) are highlighted in red. **e**, Transformation efficiency for methylated (red) or  
13 unmethylated (grey) plasmid carrying a 5'-TCAGNNNNNTCC-3' sequence, relative to a plasmid lacking this  
14 sequence.

## 1 CRISPR-Cas and MADS act in synergy

2 Given that the DMS3vir phage has already evolved to overcome the Type IE CRISPR-Cas system of the  
3 host through the *acrIE3* gene, and that it can readily evolve to overcome MADS through the acquisition  
4 of epigenetic modifications, it is unclear why the phage is unable to persist when bacteria carry both  
5 defences (Fig. 3a, black lines). To explore the reasons why this may be the case, we developed a  
6 mathematical model (see Extended Data Fig.5a and Methods for a detailed description of the model)  
7 which builds on a previous model that considered the conditions for phage amplification in the absence  
8 of phage evolution, when bacteria have CRISPR-Cas immunity and phages carry *acr* genes<sup>10</sup>. This  
9 previous model assumes that protection against CRISPR immunity provided by Acr proteins is  
10 imperfect, with the probability of a successful infection depending both on the level of host resistance  
11 ( $\rho$ ) and the efficacy of the Acr ( $\phi$ ). The model further assumes that during failed infections, some Acr  
12 proteins are produced and induce an immunosuppressed state in the surviving host, which reverts back  
13 to an immunocompetent state with rate  $\gamma^{10}$ . In order to understand how the combination of adaptive and  
14 innate defences impacts phage persistence and evolution, we modified this model to include an  
15 additional defence system that prevents phage replication with efficacy  $m$ , which phage mutants can  
16 overcome through the acquisition of epigenetic modification. As we showed previously<sup>10</sup>, if  $m=0$  (i.e.  
17 CRISPR-Cas is the only system that provides defence), the ability of phages with *acr* genes to amplify  
18 on CRISPR-Cas immune bacteria is density-dependent, with a critical threshold in phage density  
19 required for phage amplification (Fig. 4a, dark green line and ref<sup>10</sup>). However, when bacteria have both  
20 CRISPR and an additional innate immune system (i.e.  $m>0$ ), the model predicts that the critical threshold  
21 density required for phage amplification increases towards higher phage densities (Fig 4a). This is  
22 because CRISPR-immunosuppressed cells cannot be exploited as efficiently during a secondary phage  
23 infection due to the activity of the innate immune system (such as MADS). When we examine the  
24 evolution of escape phages from the innate immune system using the same model, we find that the ability  
25 of escape mutants to amplify depends on the levels CRISPR-Cas immunity, with the threshold phage  
26 density required for phage amplification shifting to higher densities as the levels of CRISPR immunity  
27 increase (increasing values of  $\rho$  in the model, Fig. 4b). This is because infections of bacteria that are  
28 more resistant to immunosuppression limit the spread of epigenetic phage mutants in the population.

29 To test the model predictions, we first validated that DMS3vir infection causes  
30 immunosuppression of the SMC4386 Type IE CRISPR-Cas system, as this assumption was based on  
31 studies using the *P. aeruginosa* PA14 model that carries a Type IF CRISPR-Cas system<sup>10,11</sup>. To test this,  
32 we briefly pre-exposed either the SMC4386-WT or the  $\Delta$ MADS strain to phage DMS3vir, washed away  
33 all phages, followed by transformation of a CRISPR-targeted or a non-targeted plasmid<sup>36</sup>. We found that  
34 the transformation efficiency of the targeted plasmid, relative to the non-targeted plasmid, increased  
35 following pre-exposure to phage DMS3vir, but not DMS3vir $\Delta$ acrIE3. This demonstrates that failed  
36 infections cause bacteria to become immunosuppressed when the phage carries the *acrIE3* gene

1 (Extended Data Fig.5b). Moreover, a similar increase in the relative transformation efficiency of the  
2 targeted plasmid was observed when bacteria encode only one (the  $\Delta$ MADS strain) or both defence  
3 systems (SMC4386-WT) (Extended Data Fig.5b). Hence, these data validate the model assumption that  
4 phages carrying *acrIE3* are imperfect in their ability to by-pass CRISPR-Cas, and that failed infections  
5 cause cells to enter into an immunosuppressed state.

6 Next, we performed infection assays over a broad range of initial phage inoculi to test that (i)  
7 phage amplification requires higher initial phage densities when both defences are present and (ii) that,  
8 in the presence of CRISPR-Cas, escape phage emergence is suppressed compared to the situation where  
9 bacteria only carry MADS. This assay revealed consistent phage amplification one day post infection  
10 (dpi), regardless of the initial phage inoculum, when bacteria lack both defence systems (i.e.,  
11  $\Delta$ CRISPR $\Delta$ MADS) (Fig. 4c). However, when bacteria only carry the CRISPR-Cas immune system (i.e.,  
12  $\Delta$ MADS), phage extinctions were observed at 1 dpi in all replicates at an initial phage inoculum of 10  
13 PFU/mL and in 5 out of 6 replicates at an initial phage inoculum of 100 PFU/mL (Fig. 4d), whereas  
14 phage amplification was observed at higher initial phage densities, consistent with previous observations  
15 that Acr-phage amplification on CRISPR-immune bacteria depends on the initial phage density<sup>10,11</sup>. In  
16 contrast, when bacteria carry only MADS (i.e.,  $\Delta$ CRISPR) we never observed phage amplification at 1  
17 dpi, even at the highest phage density ( $10^9$  PFU/mL) (Fig. 4e). Crucially, when bacteria carry both  
18 CRISPR-Cas and MADS (SMC4386-WT), we again could not observe amplification at 1 dpi across all  
19 of the initial phage inoculi (Fig. 4f). This demonstrates that at 1 dpi, phages have not yet evolved to  
20 overcome MADS, explaining why Acr-phages cannot amplify on WT bacteria.

21 However, we frequently observed later in the experiment that the phage population started to  
22 recover, but only when bacteria carried a stand-alone MADS ( $\Delta$ CRISPR) (Fig. 4g). Specifically, at 2 or  
23 3 dpi of the  $\Delta$ CRISPR strain we typically observed an increase in phage densities. Analysis of the  
24 infectivity patterns of these phages on the different host backgrounds (WT,  $\Delta$ CRISPR) revealed that this  
25 increased density was due to the emergence of escape phages that had evolved to overcome MADS (Fig.  
26 4g, red circles). Evolution of these escape phages during infection of the  $\Delta$ CRISPR strain was identified  
27 in 20 out of 42 (47%) independent experiments spanning different initial phage inoculi, from  $10^4$   
28 PFU/mL to  $10^9$  PFU/mL (corresponding to MOI of  $10^{-3}$  to  $10^2$ ). By contrast, when bacteria carried both  
29 the MADS and the CRISPR-Cas systems (i.e., SMC4386-WT), analysis of the infectivity patterns of the  
30 phage populations on the different host backgrounds (WT,  $\Delta$ CRISPR) detected escape phages in 12%  
31 of the replicates (5 out of 42) and only in experiments where the initial phage titres were very high, that  
32 is  $10^9$  PFU/mL (MOI  $10^2$ , Fig. 4h, red circles). However, recovery of phage population density was only  
33 observed in 1 out of these 5 replicates (Fig. 4h). Collectively, these experiments support the model  
34 prediction that evolution of Acr-phages to overcome MADS is suppressed when bacteria also encode a  
35 CRISPR-Cas immune system, since imperfect infectivity of Acr-phage on CRISPR-immune bacteria  
36 limits both the emergence and spread of such epigenetic mutants of the phage.

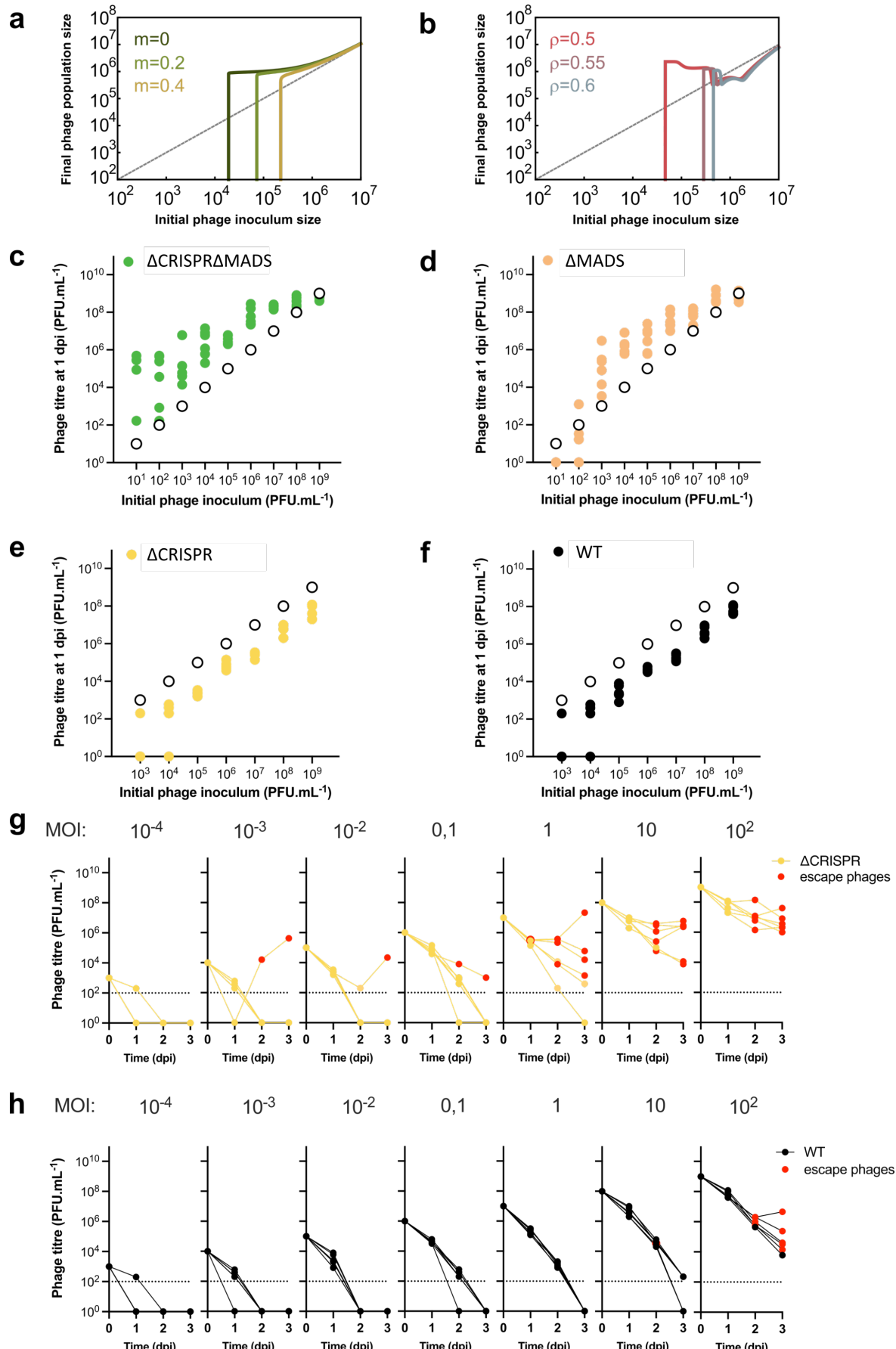


**Fig. 4 | Synergy between CRISPR-Cas and MADS.** **a**, Final phage density for different values of MADS efficacy of resistance ( $m$ ) when  $\rho = 0.6$ . **b**, Final phage density for different values of CRISPR efficacy of resistance ( $\rho$ ). In both plots the initial density of resistant cells is  $K/2$ . Other parameter values:  $m = 0.8$ ,  $r = 1$ ,  $\gamma = 20$ ,  $\phi = 0.4$ ,  $B = 5$ ,  $a = 0.001$ ,  $d = 0.001$ ,  $\lambda = 1$ ,  $\mu = 0.0001$ ,  $K = 10^6$ . **c-f**, DMS3vir titre at 1 dpi upon infection of strains that (**c**, **d**) lack or (**e**, **f**) carry MADS. Empty circles show initial phage titres and coloured

1 dots show titre at 1 dpi. **g-h**, Titre of phage DMS3vir over 3 days upon infection of strains **(g)** SMC4386ΔCRISPR  
2 and **(h)** SMC4386-WT. Each graph shows infection experiments starting with initial phage concentrations varying  
3 from  $10^3$  to  $10^9$  PFU/mL (with 10-fold increments) corresponding to initial MOIs ranging from  $10^{-4}$  to  $10^2$ . Red  
4 circles highlight replicates where escape phages could be detected. All panels show individual data for 6  
5 independent replicates.

6

## 7 Discussion

8 For the past few years, new defence systems have been discovered at unprecedented rates, suggesting  
9 that many more remain to be uncovered. These discoveries have mainly been based on computational  
10 “guilt-by-association” approaches which take advantage of the fact that defence genes often cluster  
11 together in bacterial and archaeal genomes in so-called “defence islands”<sup>14,17,23</sup>. Anti-phage genes are  
12 also frequently identified in MGE, where they form hotspots of genetic variation within the MGE<sup>37-39</sup>.  
13 In addition, these MGE tend to integrate at preferential locations in bacterial genomes, known as  
14 integration hotspots. Therefore, systematic mapping of integration hotspots and careful analyses of their  
15 gene content is becoming a valuable strategy for the discovery of the full repertoire of bacterial defence  
16 systems<sup>40-43</sup>. We now understand that bacteria encode many more defence systems than previously  
17 thought, and that individual bacterial genomes typically contain multiple defences. However, how these  
18 defences interact at the molecular, transcriptional and phenotypic levels, and how this shapes bacteria-  
19 phage coevolution remains largely unclear.

20 Here, we identify a new defence system that we named MADS in a genomic locus that is a  
21 hotspot for defence systems. MADS uses N6-methyladenosine modification of a specific recognition  
22 sequence to discriminate self from non-self DNA. We found that a bacterial strain that encodes MADS  
23 alone suppresses phage DMS3vir densities but only transiently as phages can readily acquire epigenetic  
24 modifications to escape immunity mediated by MADS. Interestingly, when bacteria also carried  
25 CRISPR-Cas immunity, phage escape evolution was rarely observed, despite the phage carrying an anti-  
26 CRISPR gene that blocks the CRISPR-Cas immune system of the host. Mathematical modelling explains  
27 why this synergy between the two defence systems emerges. It has previously been shown that phage  
28 carrying *acr* genes need to cooperate in order to overcome CRISPR immunity of their host bacteria, and  
29 this in turn causes amplification only if the initial phage densities are sufficiently high<sup>10,11</sup>. Cooperation  
30 is needed because initial infections of CRISPR immune bacteria by Acr-phages often fail, due to phage  
31 genomes being detected and destroyed by CRISPR immune complexes before they are inactivated by  
32 the Acr proteins. However, some Acr proteins will have been produced, and although the initial infection  
33 was unsuccessful, the cell enters an immunosuppressed state that can be exploited in a secondary  
34 infection (Extended Data Fig. 6). The probability that this cell will be re-infected by another Acr-phage  
35 increases with phage density, explaining the critical tipping point in Acr-phage density beyond which  
36 phage amplification is observed. However, in the presence of a second layer of defence, such as MADS,  
37 these cells with a suppressed CRISPR-Cas immune system are unavailable for phage replication. To

1 exploit these cells, phages first need to acquire the epigenetic modification to overcome MADS. The  
2 presence of CRISPR-Cas immunity limits the evolution of Acr-phage mutants that escape MADS, and  
3 even if phage mutants arise, they cannot spread as efficiently as they would in the absence of CRISPR-  
4 Cas immunity (Extended Data Fig. 6). Based on our understanding of the synergy between CRISPR-  
5 Cas and MADS upon infection with Acr-phages, we expect that similar synergistic interactions may  
6 occur between CRISPR-Cas and other innate immune systems. Future work will be needed to test this  
7 hypothesis, and if validated, to understand if and how the activity of these systems is coordinated to  
8 provide an optimal anti-phage response.

9 Collectively, our study sheds light on how multi-layered defence systems can shape bacteria-  
10 phage interactions, and shows that the coexistence of CRISPR-Cas and MADS impairs the successful  
11 deployment of phage counter-defence strategies by interfering with phage cooperation. Specifically, the  
12 presence of MADS reduces the infection success of immunosuppressed bacteria by Acr-phages, whereas  
13 the presence of the CRISPR immune system limits the emergence and spread of epigenetic mutants of  
14 the phage that overcome MADS. A more detailed understanding of the interactions between multi-  
15 layered defences and the counter-defences encoded by phages will be key to predict and manipulate  
16 bacteria-phage interactions in natural and clinical settings.

17

## 18 **Acknowledgments**

19 A.M. was supported by funding from a PhD studentship sponsored by the College of Life and  
20 Environmental Sciences (CLES, University of Exeter), and the Centre for Environment, Fisheries and  
21 Aquaculture Science (CEFAS). This work was supported by a grant from the ERC (ERC-STG-2016-  
22 714478 - EVOIMMECH), which was awarded to E.R.W. A.C. received funding from the European  
23 Union's Horizon 2020 research and innovation programme under the Marie Skłodowska-Curie grant  
24 agreement No 834052 and from IdEx Université Paris Cité (ANR 18 IDEX 0001). K. B. and C.C. drew  
25 on funding from the MRC MR/R020787/1. S.v.H. acknowledges funding from the Biotechnology and  
26 Biological Sciences Research Council (BB/S017674/1). The authors thank Dr. L. Zhang for his support  
27 in optimizing the protocol for arbitrary PCR, Dr. D. Walker-Sünderhauf for assistance in generating the  
28 transposon-mutant library, Dr. B. Watson for contributing to phage DNA isolation, Dr. A. Bernheim for  
29 feedback on building macromolecular models to detect MADS, E. Cenraud for DefenseFinder analyses,  
30 Prof. Bondy-Denomy for kindly providing phage DMS3-Gm, Prof. R. Lavigne and Dr. J. Wagemans  
31 for kindly providing phages LPB1, LMA2 and LUZ24, Prof. O'Toole for kindly providing phage  
32 DMS3vir and strain *P. aeruginosa* UCBPP-PA14 *csy3::lacZ*, and Prof. Davidson for kindly providing  
33 strain SMC4386.

34

## 35 **Declaration of interests**

36 A.M., A.C. and E.R.W. are inventors on patent GB2303034.9.

1 **Authors contributions**

2 Conceptualization, A.M., A.C. and E.R.W.; Methodology, A.M., E.P., C.C., S.G, K.B., A.C., and  
3 E.R.W.; Investigation A.M., E.P., C.C., S.G, R.C., B.J.P., M.C., A.G., S.P., K.B., S.v.H., A.C. and  
4 E.R.W.; Formal Analysis, A.M., E.P., C.C., S.G, S.P., K.B., A.C., and E.R.W.; Mathematical Modelling,  
5 S.G; Writing – Original Draft, A.M., A.C. and E.R.W.; Writing – Review & Editing, A.M., A.C. and  
6 E.R.W. with contributions from E.P., C.C., S.G., R.C., B.J.P., M.C., S.P., K.B., S.v.H.; Supervision,  
7 A.C. and E.R.W.; Funding Acquisition, E.R.W.

8

9 **Methods**

10 All experiments were carried out in six biological replicates unless otherwise specified.

11

12 **Bacterial strains**

13 *P. aeruginosa* UCBPP-PA14 *csy3::lacZ* (referred to as PA14ΔCRISPR, since it carries a disruption of  
14 an essential *cas* gene that causes the CRISPR-Cas system to be non-functional), was grown overnight at  
15 28°C or 37°C in LB broth. *P. aeruginosa* SMC4386 (referred to as SMC4386-WT), and deletion mutants  
16 of this strain (referred to as ΔCRISPR, ΔMADS, ΔCRISPRΔMADS, Δ*mad1*, Δ*mad2*, Δ*mad3*, Δ*mad4*,  
17 Δ*mad6*, Δ*mad7*, Δ*mad8*) were growth at 28°C or 37°C in either LB broth or M9 medium (22 mM  
18 Na<sub>2</sub>HPO<sub>4</sub>; 22 mM KH<sub>2</sub>PO<sub>4</sub>; 8.6 mM NaCl; 20 mM NH<sub>4</sub>Cl; 1 mM MgSO<sub>4</sub>; 0.1 mM CaCl<sub>2</sub>) supplemented  
19 with 0.2% glucose. *E. coli* MFD<sub>pir</sub> was used as donor to build the transposon mutant library, *E. coli*  
20 DH5 $\alpha$  was used to assemble the allelic exchange vectors for the gene deletions, and *E. coli* S17.1 $\lambda$ <sub>pir</sub>  
21 was used as donor strain to deliver the allelic exchange vectors to recipient cells during conjugation  
22 assays. Whenever applicable, media was supplemented with ampicillin (100  $\mu$ g/mL), streptomycin (50  
23  $\mu$ g/mL), or gentamicin (either 30  $\mu$ g/mL, when selecting for *E. coli*, or 50  $\mu$ g/mL, when selecting for *P.*  
24 *aeruginosa*) to ensure plasmid maintenance. *E. coli* MFD<sub>pir</sub> was cultured in the presence of  
25 diaminopimelic acid (DAP) (0.3 mM).

26

27 **Phage strains**

28 Recombinant temperate phage DMS3-Gm, which encodes a gentamycin resistance gene, was used to  
29 enable selection of lysogens following infection of WT and mutant SMC4386 strains as well as the  
30 transposon mutant library. Phage DMS3<sub>vir</sub>, which is obligately lytic due to the deletion of the c-  
31 repressor gene, and/or phage DMS3<sub>vir</sub>Δ*acrIE3*, which lacks both the c-repressor gene and the anti-  
32 CRISPR gene that blocks the Type IE CRISPR-Cas system of strain SMC4386, were used in all other  
33 experiments, and have been described previously<sup>28,44</sup>. Lytic phages LMA2, LUZ24 and temperate phage  
34 LPB1 were used in spot assays to determine the range of resistance conferred by MADS. Phage stocks

1 were extracted from lysates prepared on *P. aeruginosa* PA14ΔCRISPR or SMC4386ΔCRISPR and  
2 stored at 4°C.  
3

#### 4 Adsorption assay

5 The measurement of phage adsorption was performed according to Kropinsky, 2009<sup>45</sup> with some  
6 modifications. Briefly, 9 mL of *P. aeruginosa* SMC4386-WT and PA14ΔCRISPR culture (OD<sub>600</sub>=0.25)  
7 were infected with 2x10<sup>6</sup> plaque forming units (PFU)/mL of phage DMS3vir. Every 6 min for 1h, an  
8 aliquot of 100 µL was taken from each vial and transferred into a chilled Eppendorf tube containing 800  
9 µL of LB broth and 100 µL of chloroform. Extracted phages were serially diluted and spotted onto a  
10 lawn of *P. aeruginosa* PA14ΔCRISPR to determine the phage titre. The experiment was carried out in  
11 a water bath, at 28°C and with 100 rounds per minute (rpm) agitation.  
12

#### 13 Efficiency of Plaquing (EOP) assays

14 EOP assays were carried out on square polystyrene plates containing LB with 1.5% agar. A mixture of  
15 molten soft LB agar (0.5%) and 300 µL of bacteria (grown overnight in LB broth) were poured on top  
16 of the hard agar layer and allowed to set. Next, 5 µL of serially diluted phage were spotted on the  
17 resulting plates, which were subsequently incubated overnight at 28°C and plaque forming units (PFUs)  
18 were enumerated the next day. The EOP was determined as the ratio of the number of PFUs on a mutant  
19 *P. aeruginosa* SMC4386 and the *P. aeruginosa* SMC4386-WT strains. To be able to calculate the EOP  
20 with DMS3virΔacr, we arbitrarily set the phage titre on *P. aeruginosa* SMC4386-WT at 1 PFU/mL  
21 (instead of 0).  
22

#### 23 Generation of the transposon (Tn)-mutant library

24 To generate the transposon-mutant library we used the synthetic construct pBAM (born-again-mini-  
25 transposon) described by García et al., 2011<sup>46</sup>. Specifically, we utilised the vector pBAMD1-4<sup>47</sup>, which  
26 delivers the Tn5 while conferring resistance to streptomycin to the target cells at the same time, allowing  
27 for selection of transconjugants. The pBAMD1-4 vector was delivered to the recipient bacteria via  
28 conjugation using the *E. coli* MFDpir strain as donor cell, following previously described methods<sup>48</sup>.  
29 Briefly, we separately incubated 15 mL of *E. coli* MFDpir donor cells and recipients (*P. aeruginosa*  
30 SMC4386-WT and SMC4386ΔCRISPR strains), which were incubated overnight at 37°C with agitation  
31 at 180 rpm. Recipients were grown in LB broth, while donors were grown in LB broth supplemented  
32 with DAP (0.3mM), ampicillin (100 µg/mL) and streptomycin (50 µg/mL). The following day, 10 mL  
33 of each strain was pelleted and washed twice with 10 mL of M9 salts saline solution. Bacterial cultures  
34 where pelleted again and resuspended in 10 mL of LB supplemented with 0.3 mM DAP. Donors and  
35 recipient were mixed together (7500 µL donor: 500 µL recipient), pelleted and resuspended in 1 mL of  
36 M9 saline solution. To allow for conjugation between donor and recipient, 100 µL of mix was spotted

1 onto 10 individual Binder-Free Glass Microfiber 1.2  $\mu$ M filter papers (Whatman) which were placed  
2 onto a squared LB agar plate supplemented with DAP (0.3mM), and incubated at 28°C for 48h. Cells  
3 from each filter were then recovered into LB supplemented with streptomycin (to kill the non-  
4 transconjugants), pelleted, washed twice (resuspended first in 1 mL and then in 100  $\mu$ L) and plated onto  
5 an LB agar plate supplemented with streptomycin to select for the transconjugants. Plates were incubated  
6 for 24-48h at 28°C. For each recipient strain, an *E. coli* MFD<sup>pir</sup> donor strain without plasmid was used  
7 as negative control. Based on pilot data that yielded around 1000 transconjugants, this procedure was  
8 carried out in 10 independent biological replicates, which were pooled during the last step in order to  
9 obtain a saturated Tn mutant library.

10

## 11 Measuring frequencies of lysogeny

### 12 *Lysogeny in PA14 $\Delta$ CRISPR, SMC4386 and derivative knockouts strains*

13 Cultures were grown overnight at 37°C with 180 rpm agitation, in 6 mL of LB broth. Cultures were then  
14 diluted 1:100 into fresh LB broth and infected with phage DMS3-Gm<sup>49</sup> at an MOI of 0.01. After 24h,  
15 samples were serially diluted, plated onto selective (LBA with Gm) and non-selective (LBA) agar plates  
16 and incubated overnight at 28°C. Colonies were enumerated the next day. The proportion of lysogens  
17 was expressed as the number of CFU (Colony Forming Units) grown on selective plates divided by the  
18 number of CFU on non-selective media.

19

### 20 *Lysogeny in the Tn5 mutant library*

21 The transconjugants (see **Generation of the transposon (Tn)-mutant library** for details on how they  
22 were obtained) were scraped off LBA plates, pooled, and resuspended in 10 mL of LB broth and then  
23 infected with 10<sup>5</sup> PFU of phage DMS3-Gm, followed by overnight incubation at 28°C with agitation at  
24 180 rpm.

25 Each day and for 3 days, 1 mL of the culture was transferred into 10 mL of fresh LB broth, the phages  
26 were extracted to monitor phage titre and bacteria were plated onto non-selective LBA as well as LBA  
27 supplemented with streptomycin (selecting for Tn mutants) or both streptomycin and gentamicin  
28 (selecting for Tn mutants carrying the DMS3-Gm prophage). Plates were incubated at 28°C for 24-48h.  
29 Lysogenization of bacterial colonies on LBA with streptomycin and gentamicin was confirmed by  
30 colony PCR using primers Crep\_F (forward, 5'- GCGGAATGAGCGCTAAACC-3') and Crep\_R  
31 (reverse, 5'- CAAGTGCTTAGCGAGGAATGC-3'), that amplify the c-repressor gene of phage  
32 DMS3.

33

## 34 **Localization of the Tn5 insertions**

35 Before being subjected to arbitrary PCR (described below), we verified using colony PCR that the clones  
36 of interest carried the miniTn5 insertion using the primer pairs PS5 (5'-CCCTGCTTCGGGGTCATT-

1 3') and PS4 (5'-CCAGCCTCGCAGAGCAGG-3'), and PS5 and PS6 (5'-  
2 GGACAAATCCGCCGCCCT-3'), using cells carrying the plasmid pBAMD1-4 as a positive control.  
3 Both primer pairs amplify the *oriT* region of the plasmid, leading to a product size of 225 bp and 665 bp  
4 respectively. Only in case of absence of *oriT* amplification we proceeded with the arbitrary PCR. Next,  
5 we applied a protocol of arbitrary PCR to identify the location of Tn5 insertions, based on the methods  
6 described by García et al., 2014<sup>47</sup> and Saavedra et al., 2017<sup>50</sup>. In the first round of arbitrary PCR we used  
7 the forward primer ME-O-Sm-Ext-F (5'- CTTGGCCTCGCGCAGATCAG-3') and the reverse  
8 primer ARB6 (5'- GGCACCGCGTCGACTAGTACNNNNNNNNNACGCC-3'), while in the second  
9 round of arbitrary PCR we used the forward primer ME-O-Sm-Int-F (5'-  
10 CACCAAGGTAGTCGGCAAAT-3') and the reverse primer ARB2 (5'-  
11 GGCACCGCGTCGACTAGTAC-3'). We followed the PCR conditions that have been previously  
12 described<sup>47</sup>. Since all the transconjugants are different from one another (i.e., the Tn5 is in different  
13 location in the bacterial genome), some PCR conditions, such as the annealing temperature, work for  
14 some clones but not for others. Therefore, for clones where we did not obtain clear and definite bands  
15 after the second round, we adjusted the protocol as follows: in the first round the number of cycles  
16 increased from 30 to 35 and/or the annealing temperature gradually increased to a maximum of 38°C; in  
17 the second round the annealing temperature increased to 52°C. PCR products obtained after the second  
18 round of arbitrary PCR were gel purified and sent for Sanger sequencing (Eurofins Genomics UK  
19 Limited, Wolverhampton, UK). The chromatogram derived from the Sanger sequencing was mapped  
20 against the genome of *P. aeruginosa* SMC4386-WT using Geneious v10.2.6 to identify the genes where  
21 the transposon was inserted.

22

### 23 **Generation of gene knockouts**

24 The deletion of CRISPR-Cas and MADS systems, as well as the deletion of single genes from MADS  
25 were carried out using two-step allelic exchange, as described by Hmelo et al., 2015<sup>51</sup>. The homologous  
26 sequences flanking either side of the desired target system and/or gene were synthesized by Integrated  
27 DNA Technology (IDT™) or PCR amplified and fused together via SOE-PCR<sup>52,53</sup>, and then cloned into  
28 the pDONRPEX18Gm donor vector via Gateway cloning. The resulting allelic exchange vector was  
29 transformed into chemically competent *E. coli* DH5α and verified by PCR. Vectors were then  
30 electroporated into competent *E. coli* S17-1λpir to allow for conjugation with *P. aeruginosa* SMC4386-  
31 WT recipient strains<sup>51</sup>. The merodiploids that were obtained were selected on cetrizide agar plates (to  
32 select for *P. aeruginosa*) supplemented with gentamicin (50 µg/mL). Every genomic deletion was  
33 confirmed by colony PCR, first by positive amplification of the knockout junction, and then by negative  
34 amplification of the left and right side of the intact system and/or gene, followed by Sanger sequencing  
35 (Eurofins Genomics UK Limited, Wolverhampton, UK). The list of primers used to generate and screen  
36 the knockout strains are listed in Supplementary Table 4.

1

## 2 **Bioinformatic analysis of the distribution of MADS**

### 3 ***Analysis of protein domains and HMM profiles***

4 MADS locus protein sequences were determined from genome annotations made using Prokka v1.14.6,  
5 which uses Prodigal to predict protein regions. These proteins were searched against the pfam (protein  
6 family) database, as well as Phyre2 and HHpred, to perform HMM-HMM matching-based remote  
7 homology detection and obtain structural predictions<sup>54,55</sup>. Curated alignments for each gene were  
8 constructed by identifying homologues for each protein sequence using HHpred. A probability cut-off  
9 score of 50% was set, with default parameters for all other options, searching against the PDB database.  
10 Alignments extracted from HHpred outputs (max 250 sequences) were then used to generate profile-  
11 HMMs using the *hmmbuild* function from HMMER v3.0. For further investigations of remote  
12 homology, HHpred was run against the PDB, COG, NCBI conserved domains and Pfam-A databases.  
13

### 14 ***Genomes***

15 A total of 172,366 bacterial and archaeal RefSeq assemblies (retrieved January 2022 using ncbi-genome-  
16 download, <https://github.com/kblin/ncbi-genome-download/>) were downloaded for use in prevalence  
17 analysis.

18

### 19 ***Macromolecular models for MADS***

20 MacSyFinder v2, a tool for macromolecular systems detection<sup>56</sup>, was used to develop models for MADS.  
21 This tool requires the specification of mandatory or accessory components within the system, which are  
22 not biological definitions but rather describe whether a protein is easy to detect or more divergent and  
23 thus harder to detect with a single HMM profile, as well as whether components are frequently missing  
24 from systems.

25 After making sure that no known anti-phage systems could be identified by PADLOC<sup>57</sup> and  
26 DefenseFinder<sup>58</sup> within the MADS operon (Supplementary Table 1), genomes were retrieved in genbank  
27 (.gbff) format and ordered protein fasta files were created by extracting the CDS features using SeqIO  
28 from Biopython. Initial models with various levels of system completeness and genomic distance  
29 between components were tested. Initially, all *P. aeruginosa* RefSeq genomes (n=6,103) were searched.  
30 Next, preliminary tests, and manual inspection of hits from a subset of the entire Bacterial and Archaeal  
31 RefSeq dataset (n=15,000), the following model parameters were set. Proteins MAD6, 7 and 8 were  
32 defined as mandatory and their presence was required for the system to be detected. Proteins MAD1, 2  
33 and 5 were defined as accessory due to their homology to Restriction-Modification system components  
34 and widespread regulators, which could lead to false positive hits if made mandatory. Finally, proteins  
35 MAD3 and 4 were also classified as accessory, due to them not being reliably detected in all systems.  
36 In addition, the maximum inter gene distance was set to 10.

1  
2 **Taxonomic distribution and plots**  
3 Species classifications for genomes with MADS were retrieved using the Entrez python module.  
4 Taxonomic trees were retrieved from NCBI using the ete3 v3.1.2 module, and used to visualise the  
5 phylogenetic distribution of MADS. Other plots were created in R, with operons plotted using gggenes.  
6 Additional editing of plots was performed using Inkscape v1.2.  
7

8 **Reproducibility and computational resources**

9 The University of Exeter's Advanced Research Computing Facilities were used to carry out for this  
10 bioinformatics analysis. A Snakemake pipeline was used to run MacSyFinder searches on all genomes,  
11 whilst the remaining analyses were carried out using R v4.0.4 and Python version 3.9.7 with Biopython  
12 v1.79. All scripts used for this analysis are available at <https://github.com/elliekpursey/Maestri>.  
13

14 **Bioinformatic analysis of defence islands**

15 A total of 454 publicly available complete *P. aeruginosa* genomes were included in the assessment of  
16 the putative defence island (Supplementary Table 2). Defence islands were extracted from genomes by  
17 first examining the BLASTx percentage identity and genome coordinates against relevant query  
18 reference sequences of the distinct gene boundaries pheT (MPAO1\_RS11510) and a histidine kinase  
19 (MPAO1\_RS11445)<sup>59</sup>. FASTA sequence files of defence islands were extracted from complete genome  
20 FASTA files using BEDTools v2.29.2 getfasta and subtract, based upon BLASTx genome coordinates<sup>60</sup>.  
21 Prokka v1.14.6 was used to annotate defence islands and the remainder of the genome<sup>61</sup>. Defence  
22 systems in all sequence files were identified using PADLOC<sup>57</sup> and DefenseFinder<sup>58</sup>, both with  
23 additional CRISPR array detection. Wilcoxon's signed rank testing was used to determine enrichment  
24 for defence systems on the island and was performed using R v4.1.3. Manual inspection of the defence  
25 hotspots containing MADS was carried out using Geneious v10.2.6  
26

27 **Growth curves**

28 Growth curves to assess the role of MADS during infection with phage DMS3vir were performed in 96-  
29 well plates with agitation at 37°C. Briefly, overnight cultures of WT and mutant strains of *P. aeruginosa*  
30 SMC4386 grown in LB media at 37°C with agitation at 180 rpm were diluted 100-fold into fresh LB  
31 media and grown until cultures reached mid-log phase (OD600 nm of 0.3, approximately 10<sup>8</sup> CFU/mL).  
32 One mL of each mid-log culture was centrifuged for 3 min at 6000 rpm to remove the supernatant and  
33 the pellets were infected with 1 mL of DMS3vir at an MOI of 10 in LB and incubated for 10 min at 37°C  
34 whilst shaking at 180 rpm. After initial incubation to synchronise the infection, 200 µL of the infected  
35 cultures were transferred to a 96-well plate, then 20 µL of mineral oil were added on the surface of each  
36 well to avoid evaporation and bacterial growth was measured by optical density at 600 nm (OD600) for

1 24h at 37°C with agitation in a BioTek Synergy 2 plate reader. At t=0 200 µL samples were used to  
2 quantify initial bacteria CFU/mL and phage titre PFU/mL. Growth measurements in the absence of  
3 phage were carried out in parallel as a control.

4

5 **Analysis of MADS self/non-self discrimination**

6 *Infection assays in liquid medium*

7 Infection assays to measure the population dynamics of phage DMS3vir in the presence or absence of  
8 MADS were performed in glass vials by inoculating 6 mL M9 medium supplemented with 0.2% glucose  
9 with approximately  $5 \times 10^7$  CFU bacteria from fresh overnight cultures (also grown in M9 medium +  
10 0.2% glucose) of either *P. aeruginosa* SMC4386-WT strain or the isogenic  $\Delta$ CRISPR,  $\Delta$ MADS or  
11  $\Delta$ CRISPR $\Delta$ MADS strains. Cultures were infected at MOI 0.1 and 10, incubated at 37°C while shaking  
12 at 180 rpm and transferred daily (1:100 dilution) for three days into fresh medium. Phages were  
13 chloroform extracted (1:10 volume) every day and their titres measured via spot test assay onto a lawn  
14 of the sensitive *P. aeruginosa* PA14 $\Delta$ CRISPR strain. Plates were incubated overnight at 28°C. We  
15 monitored whether phages in these experiments evolved to overcome bacterial defence systems, and  
16 whether this was due to genetic or epigenetic mutations. To this end, we performed plaque-purification  
17 of phages from the SMC4386 lawns using chloroform extractions, and phage were titrated on lawns of  
18 SMC4386-WT and PA14 $\Delta$ CRISPR strains. These phages were then used in a next round of parallel  
19 infections on SMC4386-WT or PA14 $\Delta$ CRISPR strains as hosts, at 28°C in glass vials containing 6mL  
20 of LB broth, while shaking at 180 rpm. Phages were chloroform extracted again, and titrated on both  
21 strains. This process was repeated for another round of infection, to understand the heritability of the  
22 escape phenotype of the phage.

23

24 *Phage and bacteria DNA extraction for sequencing*

25 For phage DNA extraction the 4 replicate experiments of DMS3vir that during infection assays with *P.*  
26 *aeruginosa* SMC4386 $\Delta$ CRISPR (referred to as  $\Delta$ CRISPR) gained the capability to amplify after 2 days  
27 of infection (see Fig.3a), were amplified on  $\Delta$ CRISPR and  $\Delta$ CRISPR $\Delta$ mad2, which is the mutant lacking  
28 the predicted methylase, while the ancestral DMS3vir was amplified on  $\Delta$ CRISPR $\Delta$ MADS. To this end,  
29 500 µL of bacteria from a fresh overnight culture were inoculated into 50 mL of LB broth and mixed  
30 with 100 µL of an approximately  $1 \times 10^8$  PFU phage stock. Those infected cultures were grown overnight  
31 in 50 mL of broth at 28°C, 180 rpm. The resulting viscous cultures were centrifuged at 25,000 xg and  
32 phages were found to have concentrated in the pellet. The pellet was resuspended with 5 mL of phosphate  
33 buffered saline (PBS) and centrifuged at 21,000 xg to remove bacterial cells. Phages were concentrated  
34 from the supernatant using 0.5 mL 100kDa Amicon spin filters as per the manufacturers guidelines and  
35 retained in the filters. Whilst still in the filter, phages were washed twice with DNase I buffer (up to 400  
36 µL), treated with DNase I as per the manufacturers guidelines, washed twice with RNase buffer (up to

1 400 µL), treated with RNase A as per the manufacturers guidelines, washed twice with RNase buffer  
2 (up to 400 µL) and eluted from the Amicon filters by inversion and centrifugation with RNase buffer  
3 (up to 400 µL) to give a final volume for each phage solution of 400 µL. Phage DNA was extracted  
4 using a proteinase K lysis step (20 µg of proteinase K, 0.5% SDS, 20mM EDTA pH 8.0) for 1 h at 60  
5 °C followed by 2 phenol:chloroform extractions (1:1 volume, inversion and centrifugation), DNA was  
6 precipitated using sodium acetate (1/10 volume, 3M, pH 7.5 and ethanol (2.5 volume, 100%, ice-cold)  
7 overnight at -20°C. DNA was pelleted (30min, 20,000 xg, 4°C) and washed twice with ice-cold 70%  
8 ethanol, dried and resuspended in TE buffer.

9

10 For bacterial DNA extraction (*P. aeruginosa* SMC4386-WT, SMC4386ΔCRISPR,  
11 SMC4386ΔCRISPRΔMADS, SMC4386ΔCRISPRΔ*mad2*) bacteria were pelleted from overnight  
12 culture and DNA was extracted using the phenol chloroform method outlined previously. Quality  
13 Control and quantification of bacteria and phage DNA was performed with NanoDrop, Qubit and  
14 agarose gel electrophoresis; 2 µg of DNA were used for Pacific Biosciences (PacBio) sequencing  
15 (Centre For Genomic Research, Liverpool, UK).

16

### 17 ***PacBio sequencing***

18 Barcoded SMRT-Bell PacBio libraries were created from each DNA sample and run on a SMRT cell in  
19 CLR mode on a Sequel IIe platform, yielding >300,000x coverage for phage samples and 1,400 – 2,200x  
20 coverage for bacterial samples. The PacBio SMRT-Link v10.0 analysis pipeline  
21 (<https://www.pacb.com/support/software-downloads/>) was used to demultiplex samples, to detect  
22 methylation signals based on polymerase kinetics, and to identify motifs associated with methylation,  
23 all under default parameters. Resulting diagnostic plots and gff files were inspected manually. Output  
24 files, including logs, are available at [https://github.com/scottishwormboy/Maestri\\_pbio](https://github.com/scottishwormboy/Maestri_pbio). The genome  
25 reference used for DMS3 was NC\_008717.1. For SMC4386, the PacBio reads were used to create a new  
26 genome reference (accession: PRJNA905210) from the wild-type, using SMRT-Link v10.0 for  
27 microbial assembly.

28

### 29 **CRISPR immunosuppression assay**

30 CRISPR immunosuppression assays were performed as previously described<sup>36,53</sup>. This assay relies on  
31 transformation of *P. aeruginosa* SMC4386 cells with plasmid pHERD30T (non-targeted by the  
32 SMC4386 CRISPR-Cas system) and pHERD30T-cr2sp1-SMC (targeted by SMC4386 CRISPR-Cas  
33 system). Briefly, the pHERD30T-cr2sp1-SMC plasmid was constructed by inserting a 32 nucleotide  
34 protospacer matching the 1<sup>st</sup> spacer of CRISPR array 2 of the *P. aeruginosa* SMC4386 strain, flanked  
35 by the AAG Protospacer Adjacent Motif (PAM). Oligonucleotides containing the PAM and protospacer  
36 sequence (5'-agcttAAGAACCTCTACGAGCAGACCGAGTTGAAAGGGCAg-3' and 5'-

1 aattcTGCCCTTCAACTCGGTCTGCTCGTAGAGGTTCTa-3', restriction sites overhangs are  
2 indicated in small caps, protospacer in capitals and PAM underlined) were annealed to create overhangs  
3 compatible with HindIII and EcoRI, phosphorylated by T4 Polynucleotide Kinase and ligated in EcoRI-  
4 HindIII digested pHERD30T vector. Cultures of *P. aeruginosa* SMC4386-WT and isogenic  $\Delta$ CRISPR,  
5  $\Delta$ MADS and  $\Delta$ CRISPR $\Delta$ MADS strains grown overnight in 50 mL of LB medium (approximately 3.5 x  
6  $10^9$  CFU/mL) were divided in three 50 mL tubes with 10 mL of culture in each. Cells were either non-  
7 infected or infected using a final density of  $10^9$  PFU/mL (MOI=0.3) of DMS3vir or DMS3vir $\Delta$ acrIE3.  
8 After 2h of incubation at 37°C with agitation at 180 rpm, cells were harvested by centrifugation at 3500  
9 rpm for 15 minutes. A sample of the supernatant was kept for phage titration by spot assay to validate  
10 homogeneity of the phage titre across the replicates. Cells were made electrocompetent by washing them  
11 twice with 1 mL of 300 mM sucrose solution at room temperature and resuspended in 300  $\mu$ L of the  
12 same solution. A 100  $\mu$ L sample of the resuspended cells was taken to evaluate the bacterial density.  
13 The remaining 200  $\mu$ L were equally divided across two vials and electroporated with 500 ng of either  
14 pHERD30T or pHERD30T-cr2sp1-SMC, followed by addition of 700  $\mu$ L fresh LB medium. After  
15 incubating for 1h at 37°C at 180 rpm, bacteria were pelleted, resuspended in 100  $\mu$ L of LB medium and  
16 serially diluted in LB-medium. Fifty microliters of each dilution were spotted on LB agar plates  
17 containing Gentamycin (50  $\mu$ g/mL) and incubated overnight at 37°C to allow transformants to grow.  
18 Relative transformation efficiency was calculated as the number of colonies obtained after  
19 transformation with pHERD30T-cr2sp1-SMC divided by the number of colonies obtained after  
20 transformation with pHERD30T.

21

## 22 **Plasmid transformation assay**

23 This assay was adapted from the CRISPR immunosuppression assay to fit the MADS. It relies on  
24 transformation of *P. aeruginosa* SMC4386 cells with plasmid pHERD30T (non-targeted by the  
25 SMC4386 MADS) and pHERD30T-M24 (targeted by SMC4386 MADS). Briefly, the pHERD30T-M24  
26 plasmid was constructed by inserting a 11 nucleotide MADS target sequence (5'-TCAGCGCGTCC-3').  
27 Oligonucleotides containing the target sequence (5'-agttTCAGCGCGTCCg-3' and 5'-  
28 aattcGGACGCGCTGAa-3', restriction sites overhangs are indicated in small caps and target sequence  
29 in capitals) were annealed to create overhangs compatible with HindIII and EcoRI, phosphorylated by  
30 T4 Polynucleotide Kinase and ligated in EcoRI-HindIII digested pHERD30T vector. Each of the two  
31 plasmids were then transformed in either *P. aeruginosa* SMC4386 $\Delta$ CRISPR $\Delta$ MADS or isogenic  
32  $\Delta$ CRISPR $\Delta$ mad3. These transformed strains were then used for plasmid production, which were purified  
33 with GeneJET Plasmid Midiprep kit (Thermo Scientific, USA) according to the manufacturer's  
34 instructions. Plasmid produced in *P. aeruginosa* SMC4386 $\Delta$ CRISPR $\Delta$ MADS were called pHERD30T-  
35 Nonmeth and pHERD30T-M24-Nonmeth, while plasmids produced in *P. aeruginosa*  
36 SMC4386 $\Delta$ CRISPR $\Delta$ mad3 were called pHERD30T-Meth and pHERD30T-M24-Meth.

1 Cultures of *P. aeruginosa* SMC4386-WT and isogenic  $\Delta$ CRISPR,  $\Delta$ MADS and  $\Delta$ CRISPR $\Delta$ MADS  
2 strains grown overnight in 20 mL of LB medium (approximately  $3.5 \times 10^9$  CFU/mL) were harvested by  
3 centrifugation at 3500 rpm for 15 minutes. Cells were made electrocompetent by washing them twice  
4 with 2 mL of 300 mM sucrose solution at room temperature and resuspended in 500  $\mu$ L of the same  
5 solution. A 100  $\mu$ L sample of the resuspended cells was taken to evaluate the bacterial density. The  
6 remaining 400  $\mu$ L were equally divided across four vials and electroporated with 500 ng of either  
7 pHERD30T-Nonmeth, pHERD30T-M24-Nonmeth, pHERD30T-Meth or pHERD30T-M24-Meth,  
8 followed by addition of 700  $\mu$ L fresh LB medium. After incubating for 1h at 37°C at 180 rpm, bacteria  
9 were pelleted, resuspended in 100  $\mu$ L of LB medium and serially diluted in LB-medium. Fifty  
10 microliters of each dilution were spotted on LB agar plates containing Gentamycin (50  $\mu$ g/mL) and  
11 incubated overnight at 37°C to allow transformants to grow. Relative transformation efficiency of  
12 methylated or non-methylated plasmids (respectively) were calculated as the number of colonies  
13 obtained after transformation with pHERD30T-M24-Nonmeth or pHERD30T-M24-Meth divided by  
14 the number of colonies obtained after transformation with pHERD30T-Nonmeth or pHERD30T-Meth,  
15 respectively.

16

## 17 **Phenotypic interactions between CRISPR-Cas and MADS**

### 18 *Tipping-point assay*

19 Infection assays were performed in glass vials by inoculating 6 mL M9 medium supplemented with  
20 0.2% glucose with approximately  $10^7$  CFU bacteria from fresh overnight cultures (also grown in M9  
21 medium + 0.2% glucose) of the *P. aeruginosa* SMC4386-WT strain and the isogenic  $\Delta$ CRISPR,  
22  $\Delta$ MADS and  $\Delta$ CRISPR $\Delta$ MADS strains. To these vials, phage DMS3vir was added at a MOI of  $10^{-4}$ ,  $10^{-3}$ ,  
23  $10^{-2}$ ,  $10^{-1}$ , 1,  $10^1$ , or  $10^2$ , and incubated at 37°C while shaking at 180 rpm. Cultures were transferred  
24 daily (1:100 dilution) for three days into fresh M9 medium. For the *P. aeruginosa* SMC4386 $\Delta$ MADS  
25 and the SMC4386 $\Delta$ CRISPR $\Delta$ MADS strains we performed additional infections at MOI  $10^{-5}$  and MOI  
26  $10^{-6}$  for seven days. Phages were chloroform extracted every day and the titres were measured using spot  
27 assays onto lawns of each of the four different bacterial strains (i.e., *P. aeruginosa* SMC4386-WT,  
28  $\Delta$ CRISPR,  $\Delta$ MADS and  $\Delta$ CRISPR $\Delta$ MADS strains). Plates were incubated overnight at 28°C.

29 To identify replicate experiments in which phage mutants had emerged that escape MADS, we  
30 determined for each phage sample the EOP ratio's on *P. aeruginosa* SMC4386 $\Delta$ CRISPR $\Delta$ MADS and  
31 either the  $\Delta$ CRISPR or WT bacteria. For WT DMS3vir phages, these ratios are  $127 \pm 17$  and  $142 \pm 33$   
32 (mean  $\pm$  95% c.i.), respectively. For clonal phage populations of DMS3vir escape mutants (carrying the  
33 epigenetic modification to overcome MADS), these ratios are  $0.91 \pm 0.15$  and  $1.18 \pm 0.12$  (mean  $\pm$  95%  
34 c.i.), respectively. We therefore applied a conservative threshold of EOP=5 (i.e. corresponding to  $\pm 20\%$   
35 escape mutants in the phage population) to identify samples that contained significant numbers of

1 MADS escape phages. Replicates where escape phages were detected are depicted as red circles in  
2 Figure 4 g, h.

3

4 **Mathematical modelling**

5 ***Epidemiological dynamics (no phage evolution)***

6 We develop a model to understand the dynamics of bacteriophages in a multiresistant bacteria  
7 population. Earlier studies have examined the evolution of Acr in well-mixed environments<sup>44,62</sup>. Here,  
8 we explore how the addition of a second resistance could affect the dynamics.

9 Extended Data Fig.5a shows a schematic representation of the phage life cycle (where we assume that  
10 bacteria are initially CRISPR resistant to the phage). The Acr-phage is able to infect resistant bacteria  
11 with a probability  $1 - \rho$ , where  $\rho$  is a measure of CRISPR efficiency. These infections can either lead  
12 in (i) the production of immunosuppressed cells with probability  $r(1 - \phi)$ , where  $r$  is another measure  
13 of CRISPR efficiency and  $\phi$  is a measure of anti-CRISPR efficiency, or (ii) they can result in cell lysis  
14 and the release of  $B$  virions with probability  $(1 - r(1 - \phi))(1 - m)$ , where  $m$  is a measure of MADS  
15 efficiency.

16 This yields the following system of ordinary differential equations (where  $N = R + S$ ):

17

$$\begin{aligned} \frac{dR}{dt} &= \lambda R \left(1 - \frac{N}{K}\right) - aV(1 - \rho) \left(1 - (1 - e)m(1 - r(1 - \phi))\right) R - dR + \gamma S \\ \frac{dS}{dt} &= a(1 - \rho)r(1 - \phi)RV - aV(1 - (1 - e)m)S - dS - \gamma S \\ \frac{dV}{dt} &= \left( aB \left( (1 - \rho)(1 - (1 - e)m)(1 - r(1 - \phi))R + (1 - (1 - e)m)S \right. \right. \\ &\quad \left. \left. - aN \right) V \right) \end{aligned} \quad (1)$$

18 The change in the total density of virus  $V$  at the beginning of an epidemic where  $S = 0$  and  $N = R$ :

19

$$\frac{dV}{dt} = aN(B(1 - \rho)(1 - (1 - e)m)(1 - r(1 - \phi)) - 1)V$$

21

22 In other words, the phage population can grow only when:

$$\phi > \phi_0 = \frac{1}{B(1 - \rho)(1 - (1 - e)m)r} - \frac{1 - r}{r}$$

24

25 Yet, if one introduces a large density of phages in the host population they will immunosuppress a  
26 fraction  $S/N$  of the cells. This will yield the following threshold

27

1 
$$\phi > \phi_0 - \frac{S}{R} (B(1 - (1 - e)m) - 1) \left( \phi_0 + \left( \frac{1 - r}{r} \right) \right)$$

2

3 In other words, we recover the results of ref<sup>62</sup> (in the case where  $m = 0$ ) and extend it to the case where  
4 bacteria carry the MADS resistance. The above expression shows that increasing  $m$  always increases  
5 the threshold density of viruses above which the epidemic can take off (see Fig. 4a).

6

7 ***Evolutionary dynamics of the phage (MADS escape)***

8 In the following we consider an alternative model where the phage can acquire an epigenetic mutation  
9 allowing the virus to escape MADS (i.e., the parameter  $e = 1$  for the escape mutant):

$$\begin{aligned} \frac{dR}{dt} &= rR \left( 1 - \frac{N}{K} \right) - a(1 - \rho)R \left( (1 - (1 - e)m(1 - r(1 - \phi)))V + V^e \right) - dR + \gamma S \\ \frac{dS}{dt} &= a(1 - \rho)r(1 - \phi)R(V + V^e) - a((1 - (1 - e)m)V + V^e)S - (d + \gamma)S \\ \frac{dV}{dt} &= \left( aB(1 - (1 - e)m)(1 - \rho)(1 - r(1 - \phi))R + S \right) - aN \right) V - \mu V \\ \frac{dV^e}{dt} &= \left( aB((1 - \rho)(1 - r(1 - \phi))R + S) - aN \right) V^e + \mu V \end{aligned} \tag{2}$$

10 We use this model to explore what happens if we allow some mutation to occur between  $V$  and  $V^e$  (i.e.,  
11  $\mu = 0.0001$ ), showing that the tipping point for phage amplification shifts to higher initial phage  
12 densities as the strength of CRISPR immunity increases (see Fig 4b).

13 Another way to formalise the evolution of escape mutation (focusing on the frequency  $f^e$  of the mutant)  
14 where  $f^e$  is the frequency of the mutated virus:

15 
$$f^e = \frac{V^e}{V^T}$$

16 with  $V^T = V^e + V$  and:

17

18 
$$\frac{dV^T}{dt} = \left( aB((1 - \rho)(1 - r(1 - \phi))R + S)(1 - (1 - f^e)(1 - e)m) - aN \right) V^T$$

19

20 In other words, the phage population  $V^T$  can only grow when:

21

22 
$$\phi > \phi_0 = \frac{1}{B(1 - \rho)(1 - (1 - f^e)(1 - e)m)r} - \frac{1 - r}{r}$$

23

24 Yet, if one introduces a large density of phages in the host population they will immunosuppress a  
25 fraction  $S/N$  of the cells. This will yield the following threshold

1

$$2 \quad \phi > \phi_0 - \frac{S}{R} (B(1 - (1 - f^e)(1 - e)m) - 1) \left( \phi_0 + \left( \frac{1 - r}{r} \right) \right)$$

3

4 The change in mutant frequency is:

5

$$6 \quad \frac{df^e}{dt} = \underbrace{f^e(1 - f^e)}_{\text{genetic variance}} \underbrace{aB \left( (1 - \rho)(1 - r(1 - \phi))R + S \right) (1 - e)m}_{\text{coefficient of selection}} \quad (2)$$

7

8 The equation (2) captures what parameters govern the speed at which the mutant virus is expected to  
9 increase in frequency. In particular, higher  $m$  (stronger MADS), higher  $\phi$  (stronger Acr), lower  $\rho$  or  $r$   
10 (less effective CRISPR resistance, i.e., lower numbers of spacers in the CRISPR array) promote the  
11 evolution of the mutant virus. Besides, the parameter  $\gamma$  may also affect the strength of selection via its  
12 effect on the quantity of  $R$  cells. When  $\gamma$  is large, the immunosuppressed cells recover their immunity  
13 very fast, the density  $R$  increases which favors the increase in  $V^e$  frequency.

14

## 15 **Data availability**

16 Source data associated with main figures and Extended Data Figures will be provided prior publication.  
17 Ordinary differential equations generated for mathematical modelling are included in Methods.  
18 Sequencing data have been deposited in NCBI under the BioProject accession number PRJNA905210.

19

## 20 **Code availability**

21 Bacterial and archaeal RefSeq assemblies and scripts used to carry out bioinformatic analyses are  
22 publicly available as indicated in Methods and Supplementary Tables.

23

24

25

1 **References**

- 2 1. Tal, N., and Sorek, R. (2022). SnapShot: Bacterial immunity. *Cell* *185*, 578-578.e1. 10.1016/j.cell.2021.12.029.
- 4 2. Millman, A., Melamed, S., Leavitt, A., Doron, S., Bernheim, A., Hör, J., Lopatina, A., Ofir, G., Hochhauser, D., Stokar-Avihail, A., et al. (2022). An expanding arsenal of immune systems that 5 protect bacteria from phages (Microbiology) 10.1101/2022.05.11.491447.
- 7 3. Tesson, F., Hervé, A., Mordret, E., Touchon, M., d'Humières, C., Cury, J., and Bernheim, A. 8 (2022). Systematic and quantitative view of the antiviral arsenal of prokaryotes. *Nat. Commun.* *13*, 9 2561. 10.1038/s41467-022-30269-9.
- 10 4. Tesson, F., and Bernheim, A. (2023). Synergy and regulation of antiphage systems: toward the 11 existence of a bacterial immune system? *Curr. Opin. Microbiol.* *71*, 102238. 12 10.1016/j.mib.2022.102238.
- 13 5. Spoerel, N., Herrlich, P., and Bickle, T. (1979). A novel bacteriophage defence mechanism: the 14 anti-restriction protein. *Nature* *278*, 30–34. <https://doi.org/10.1038/278030a0>.
- 15 6. Bondy-Denomy, J., Pawluk, A., Maxwell, K.L., and Davidson, A.R. (2013). Bacteriophage genes 16 that inactivate the CRISPR/Cas bacterial immune system. *Nature* *493*, 429–432. 17 10.1038/nature11723.
- 18 7. Huiting, E., Athukoralage, J., Guan, J., Silas, S., Carion, H., and Bondy-Denomy, J. (2022). 19 Bacteriophages antagonize cGAS-like immunity in bacteria (Microbiology) 20 10.1101/2022.03.30.486325.
- 21 8. Hobbs, S.J., Wein, T., Lu, A., Morehouse, B.R., Schnabel, J., Leavitt, A., Yirmiya, E., Sorek, R., 22 and Kranzusch, P.J. (2022). Phage anti-CBASS and anti-Pycsar nucleases subvert bacterial 23 immunity. *Nature* *605*, 522–526. 10.1038/s41586-022-04716-y.
- 24 9. Ho, P., Chen, Y., Biswas, S., Canfield, E., and Feldman, D.E. (2022). Bacteriophage anti-defense 25 genes that neutralize TIR and STING immune responses (Microbiology) 26 10.1101/2022.06.09.495361.
- 27 10. Landsberger, M., Gandon, S., Meaden, S., Rollie, C., Chevallereau, A., Chabas, H., Buckling, A., 28 Westra, E.R., and van Houte, S. (2018). Anti-CRISPR Phages Cooperate to Overcome CRISPR- 29 Cas Immunity. *Cell* *174*, 908-916.e12. 10.1016/j.cell.2018.05.058.
- 30 11. Borges, A.L., Zhang, J.Y., Rollins, M.F., Osuna, B.A., Wiedenheft, B., and Bondy-Denomy, J. 31 (2018). Bacteriophage Cooperation Suppresses CRISPR-Cas3 and Cas9 Immunity. *Cell* *174*, 917- 32 925.e10. 10.1016/j.cell.2018.06.013.
- 33 12. Chevallereau, A., Pons, B.J., van Houte, S., and Westra, E.R. (2022). Interactions between 34 bacterial and phage communities in natural environments. *Nat. Rev. Microbiol.* *20*, 49–62. 35 10.1038/s41579-021-00602-y.
- 36 13. Dimitriu, T., Szczelkun, M.D., and Westra, E.R. (2020). Evolutionary Ecology and Interplay of 37 Prokaryotic Innate and Adaptive Immune Systems. *Curr. Biol.* *30*, R1189–R1202. 38 10.1016/j.cub.2020.08.028.
- 39 14. Doron, S., Melamed, S., Ofir, G., Leavitt, A., Lopatina, A., Keren, M., Amitai, G., and Sorek, R. 40 (2018). Systematic discovery of antiphage defense systems in the microbial pangenome. *Science* 41 359, eaar4120. 10.1126/science.aar4120.

1 15. Cohen, D., Melamed, S., Millman, A., Shulman, G., Oppenheimer-Shaanan, Y., Kacen, A., Doron,  
2 S., Amitai, G., and Sorek, R. (2019). Cyclic GMP–AMP signalling protects bacteria against viral  
3 infection. *Nature* *574*, 691–695. 10.1038/s41586-019-1605-5.

4 16. Millman, A., Bernheim, A., Stokar-Avihail, A., Fedorenko, T., Voichek, M., Leavitt, A.,  
5 Oppenheimer-Shaanan, Y., and Sorek, R. (2020). Bacterial Retrons Function In Anti-Phage  
6 Defense. *Cell* *183*, 1551-1561.e12. 10.1016/j.cell.2020.09.065.

7 17. Gao, L., Altae-Tran, H., Böhning, F., Makarova, K.S., Segel, M., Schmid-Burgk, J.L., Koob, J.,  
8 Wolf, Y.I., Koonin, E.V., and Zhang, F. (2020). Diverse enzymatic activities mediate antiviral  
9 immunity in prokaryotes. *Science* *369*, 1077–1084. 10.1126/science.aba0372.

10 18. Tal, N., Morehouse, B.R., Millman, A., Stokar-Avihail, A., Avraham, C., Fedorenko, T., Yirmiya,  
11 E., Herbst, E., Brandis, A., Mehlman, T., et al. (2021). Cyclic CMP and cyclic UMP mediate  
12 bacterial immunity against phages. *Cell* *184*, 5728-5739.e16. 10.1016/j.cell.2021.09.031.

13 19. Bernheim, A., Millman, A., Ofir, G., Meitav, G., Avraham, C., Shomar, H., Rosenberg, M.M., Tal,  
14 N., Melamed, S., Amitai, G., et al. (2021). Prokaryotic viperins produce diverse antiviral  
15 molecules. *Nature* *589*, 120–124. 10.1038/s41586-020-2762-2.

16 20. Makarova, K.S., Wolf, Y.I., Snir, S., and Koonin, E.V. (2011). Defense Islands in Bacterial and  
17 Archaeal Genomes and Prediction of Novel Defense Systems. *J. Bacteriol.* *193*, 6039–6056.  
18 10.1128/JB.05535-11.

19 21. Makarova, K.S., Wolf, Y.I., and Koonin, E.V. (2013). Comparative genomics of defense systems  
20 in archaea and bacteria. *Nucleic Acids Res.* *41*, 4360–4377. 10.1093/nar/gkt157.

21 22. Oliveira, P.H., Touchon, M., and Rocha, E.P.C. (2014). The interplay of restriction-modification  
22 systems with mobile genetic elements and their prokaryotic hosts. *Nucleic Acids Res.* *42*, 10618–  
23 10631. 10.1093/nar/gku734.

24 23. Bernheim, A., and Sorek, R. (2020). The pan-immune system of bacteria: antiviral defence as a  
25 community resource. *Nat. Rev. Microbiol.* *18*, 113–119. 10.1038/s41579-019-0278-2.

26 24. Picton, D.M., Luyten, Y.A., Morgan, R.D., Nelson, A., Smith, D.L., Dryden, D.T.F., Hinton,  
27 J.C.D., and Blower, T.R. (2021). The phage defence island of a multidrug resistant plasmid uses  
28 both BREX and type IV restriction for complementary protection from viruses. *Nucleic Acids Res.*  
29 *49*, 11257–11273. 10.1093/nar/gkab906.

30 25. Dupuis, M.-È., Villion, M., Magadán, A.H., and Moineau, S. (2013). CRISPR-Cas and restriction–  
31 modification systems are compatible and increase phage resistance. *Nat. Commun.* *4*, 2087.  
32 10.1038/ncomms3087.

33 26. Hynes, A.P., Villion, M., and Moineau, S. (2014). Adaptation in bacterial CRISPR-Cas immunity  
34 can be driven by defective phages. *Nat. Commun.* *5*, 4399. 10.1038/ncomms5399.

35 27. Maguin, P., Varble, A., Modell, J.W., and Marraffini, L.A. (2022). Cleavage of viral DNA by  
36 restriction endonucleases stimulates the type II CRISPR-Cas immune response. *Mol. Cell* *82*, 907–  
37 919.e7. 10.1016/j.molcel.2022.01.012.

38 28. Cady, K.C., Bondy-Denomy, J., Heussler, G.E., Davidson, A.R., and O'Toole, G.A. (2012). The  
39 CRISPR/Cas Adaptive Immune System of *Pseudomonas aeruginosa* Mediates Resistance to  
40 Naturally Occurring and Engineered Phages. *J. Bacteriol.* *194*, 5728–5738. 10.1128/JB.01184-12.

1 29. Pawluk, A., Bondy-Denomy, J., Cheung, V.H.W., Maxwell, K.L., and Davidson, A.R. (2014). A  
2 New Group of Phage Anti-CRISPR Genes Inhibits the Type I-E CRISPR-Cas System of  
3 *Pseudomonas aeruginosa*. *mBio* 5, e00896-14. 10.1128/mBio.00896-14.

4 30. Rollie, C., Chevallereau, A., Watson, B.N.J., Chyou, T., Fradet, O., McLeod, I., Fineran, P.C.,  
5 Brown, C.M., Gandon, S., and Westra, E.R. (2020). Targeting of temperate phages drives loss of  
6 type I CRISPR-Cas systems. *Nature* 578, 149–153. 10.1038/s41586-020-1936-2.

7 31. Taboada, B., Estrada, K., Ciria, R., and Merino, E. (2018). Operon-mapper: a web server for  
8 precise operon identification in bacterial and archaeal genomes. *Bioinformatics* 34, 4118–4120.  
9 10.1093/bioinformatics/bty496.

10 32. Coppens, L., and Lavigne, R. (2020). SAPPHIRE: a neural network based classifier for  $\sigma$ 70  
11 promoter prediction in *Pseudomonas*. *BMC Bioinformatics* 21, 415. 10.1186/s12859-020-03730-z.

12 33. Payne, L.J., Meaden, S., Mestre, M.R., Palmer, C., Toro, N., Fineran, P.C., and Jackson, S.A.  
13 (2022). PADLOC: a web server for the identification of antiviral defence systems in microbial  
14 genomes. *Nucleic Acids Res.* 50, W541–W550. 10.1093/nar/gkac400.

15 34. Abby, S.S., Néron, B., Ménager, H., Touchon, M., and Rocha, E.P.C. (2014). MacSyFinder: A  
16 Program to Mine Genomes for Molecular Systems with an Application to CRISPR-Cas Systems.  
17 *PLoS ONE* 9, e110726. 10.1371/journal.pone.0110726.

18 35. Hampton, H.G., Watson, B.N.J., and Fineran, P.C. (2020). The arms race between bacteria and  
19 their phage foes. *Nature* 577, 327–336. 10.1038/s41586-019-1894-8.

20 36. Pons, B.J., Westra, E.R., and van Houte, S. (2023). Determination of Acr-mediated  
21 immunosuppression in *Pseudomonas aeruginosa*. *MethodsX* 10, 101941.  
22 10.1016/j.mex.2022.101941.

23 37. Hussain, F.A., Dubert, J., Elsherbini, J., Murphy, M., VanInsberghe, D., Arevalo, P., Kauffman,  
24 K., Rodino-Janeiro, B.K., Gavin, H., Gomez, A., et al. (2021). Rapid evolutionary turnover of  
25 mobile genetic elements drives bacterial resistance to phages. *Science* 374, 488–492.  
26 10.1126/science.abb1083.

27 38. Rousset, F., Dowding, J., Bernheim, A., Rocha, E.P.C., and Bikard, D. (2021). Prophage-encoded  
28 hotspots of bacterial immune systems (*Microbiology*) 10.1101/2021.01.21.427644.

29 39. Fillol-Salom, A., Rostøl, J.T., Ojiogu, A.D., Chen, J., Douce, G., Humphrey, S., and Penadés, J.R.  
30 (2022). Bacteriophages benefit from mobilizing pathogenicity islands encoding immune systems  
31 against competitors. *Cell* 185, 3248–3262.e20. 10.1016/j.cell.2022.07.014.

32 40. Johnson, M.C., Laderman, E., Huiting, E., Zhang, C., Davidson, A., and Bondy-Denomy, J.  
33 (2022). Core Defense Hotspots within *Pseudomonas aeruginosa* are a consistent and rich source of  
34 anti-phage defense systems. 2022.11.11.516204. 10.1101/2022.11.11.516204.

35 41. Vassallo, C.N., Doering, C.R., Littlehale, M.L., Teodoro, G.I.C., and Laub, M.T. (2022). A  
36 functional selection reveals previously undetected anti-phage defence systems in the *E. coli*  
37 pangenome. *Nat. Microbiol.* 7, 1568–1579. 10.1038/s41564-022-01219-4.

38 42. Hochhauser, D., Millman, A., and Sorek, R. (2022). The defence island repertoire of the  
39 *Escherichia coli* pan-genome (*Microbiology*) 10.1101/2022.06.09.495481.

40 43. Benler, S., Faure, G., Altae-Tran, H., Shmakov, S., Zhang, F., and Koonin, E. (2021). Cargo Genes  
41 of Tn7-Like Transposons Comprise an Enormous Diversity of Defense Systems, Mobile Genetic  
42 Elements, and Antibiotic Resistance Genes. 12, 20.

1 44. Chevallereau, A., Meaden, S., Fradet, O., Landsberger, M., Maestri, A., Biswas, A., Gandon, S.,  
2 van Houte, S., and Westra, E.R. (2020). Exploitation of the Cooperative Behaviors of Anti-  
3 CRISPR Phages. *Cell Host Microbe* 27, 189–198.e6. 10.1016/j.chom.2019.12.004.

4 45. Clokie, M.R.J., and Kropinski, A.M. eds. (2009). *Bacteriophages* (Humana Press) 10.1007/978-1-  
5 60327-164-6.

6 46. Martínez-García, E., Calles, B., Arévalo-Rodríguez, M., and de Lorenzo, V. (2011). pBAM1: an  
7 all-synthetic genetic tool for analysis and construction of complex bacterial phenotypes. *BMC*  
8 *Microbiol.* 11, 38. 10.1186/1471-2180-11-38.

9 47. Martínez-García, E., Aparicio, T., de Lorenzo, V., and Nikel, P.I. (2014). New Transposon Tools  
10 Tailored for Metabolic Engineering of Gram-Negative Microbial Cell Factories. *Front. Bioeng.*  
11 *Biotechnol.* 2. 10.3389/fbioe.2014.00046.

12 48. Ferrières, L., Hémery, G., Nham, T., Guérout, A.-M., Mazel, D., Beloin, C., and Ghigo, J.-M.  
13 (2010). Silent Mischief: Bacteriophage Mu Insertions Contaminate Products of *Escherichia coli*  
14 Random Mutagenesis Performed Using Suicidal Transposon Delivery Plasmids Mobilized by  
15 Broad-Host-Range RP4 Conjugative Machinery. *J. Bacteriol.* 192, 6418–6427. 10.1128/JB.00621-  
16 10.

17 49. Borges, A.L., Zhang, J.Y., Rollins, M.F., Osuna, B.A., Wiedenheft, B., and Bondy-Denomy, J.  
18 (2018). Bacteriophage Cooperation Suppresses CRISPR-Cas3 and Cas9 Immunity. *Cell* 174, 917–  
19 925.e10. 10.1016/j.cell.2018.06.013.

20 50. Saavedra, J.T., Schwartzman, J.A., and Gilmore, M.S. (2017). Mapping Transposon Insertions in  
21 Bacterial Genomes by Arbitrarily Primed PCR. *Curr. Protoc. Mol. Biol.* 118. 10.1002/cpmb.38.

22 51. Hmelo, L.R., Borlee, B.R., Almblad, H., Love, M.E., Randall, T.E., Tseng, B.S., Lin, C., Irie, Y.,  
23 Storek, K.M., Yang, J.J., et al. (2015). Precision-engineering the *Pseudomonas aeruginosa* genome  
24 with two-step allelic exchange. *Nat. Protoc.* 10, 1820–1841. 10.1038/nprot.2015.115.

25 52. Horton, R.M., Hunt, H.D., Ho, S.N., Pullen, J.K., and Pease, L.R. (1989). Engineering hybrid  
26 genes without the use of restriction enzymes: gene splicing by overlap extension. *Gene* 77, 61–68.  
27 10.1016/0378-1119(89)90359-4.

28 53. Horton, R.M., Cai, Z., Ho, S.N., and Pease, L.R. (2013). Gene Splicing by Overlap Extension:  
29 Tailor-Made Genes Using the Polymerase Chain Reaction. *BioTechniques* 54, 129–133.  
30 10.2144/000114017.

31 54. Zimmermann, L., Stephens, A., Nam, S.-Z., Rau, D., Kübler, J., Lozajic, M., Gabler, F., Söding,  
32 J., Lupas, A.N., and Alva, V. (2018). A Completely Reimplemented MPI Bioinformatics Toolkit  
33 with a New HHpred Server at its Core. *J. Mol. Biol.* 430, 2237–2243. 10.1016/j.jmb.2017.12.007.

34 55. Kelley, L.A., Mezulis, S., Yates, C.M., Wass, M.N., and Sternberg, M.J.E. (2015). The Phyre2  
35 web portal for protein modeling, prediction and analysis. *Nat. Protoc.* 10, 845–858.  
36 10.1038/nprot.2015.053.

37 56. Abby, S.S., Néron, B., Ménager, H., Touchon, M., and Rocha, E.P.C. (2014). MacSyFinder: A  
38 Program to Mine Genomes for Molecular Systems with an Application to CRISPR-Cas Systems.  
39 *PLoS ONE* 9, e110726. 10.1371/journal.pone.0110726.

40 57. Payne, L.J., Meaden, S., Mestre, M.R., Palmer, C., Toro, N., Fineran, P.C., and Jackson, S.A.  
41 (2022). PADLOC: a web server for the identification of antiviral defence systems in microbial  
42 genomes. *Nucleic Acids Res.* 50, W541–W550. 10.1093/nar/gkac400.

1 58. Tesson, F., Hervé, A., Mordret, E., Touchon, M., d’Humières, C., Cury, J., and Bernheim, A.  
2 (2022). Systematic and quantitative view of the antiviral arsenal of prokaryotes. *Nat. Commun.* *13*,  
3 2561. 10.1038/s41467-022-30269-9.

4 59. Altschul, S.F., Gish, W., Miller, W., Myers, E.W., and Lipman, D.J. (1990). Basic Local  
5 Alignment Search Tool. *J. Mol. Biol.* *215*, 8. [https://doi.org/10.1016/S0022-2836\(05\)80360-2](https://doi.org/10.1016/S0022-2836(05)80360-2).

6 60. Quinlan, A.R., and Hall, I.M. (2010). BEDTools: a flexible suite of utilities for comparing  
7 genomic features. *Bioinformatics* *26*, 841–842. 10.1093/bioinformatics/btq033.

8 61. Seemann, T. (2014). Prokka: rapid prokaryotic genome annotation. *Bioinformatics* *30*, 2068–2069.  
9 10.1093/bioinformatics/btu153.

10 62. Landsberger, M., Gandon, S., Meaden, S., Rollie, C., Chevallereau, A., Chabas, H., Buckling, A.,  
11 Westra, E.R., and van Houte, S. (2018). Anti-CRISPR Phages Cooperate to Overcome CRISPR-  
12 Cas Immunity. *Cell* *174*, 908-916.e12. 10.1016/j.cell.2018.05.058.

13